universität wien

MASTERARBEIT / MASTER'S THESIS

Titel der Masterarbeit / Title of the Master's Thesis

Synthesis and characterization of precursor molecules for fluorine-18 labelled PET radiopharmaceuticals

verfasst von / submitted by

Romana Langsenlehner, BSc

angestrebter akademischer Grad / in partial fulfilment of the requirements for the degree of

Magistra pharmaciae (Mag.pharm.)

Wien, 2024 / Vienna, 2024

Studienkennzahl lt. Studienblatt / degree programme code as it appears on the student record sheet:	UA 066 605
Studienrichtung lt. Studienblatt / degree programme as it appears on the student record sheet:	Masterstudium Pharmazie
Betreut von / Supervisor:	Ass. Prof. Mag. Dr. Verena Pichler

Acknowledgements

I would like to take this opportunity to express my deep appreciation to those who have supported me during my master's thesis and all throughout my academic journey.

First and foremost, I would like to express my deepest gratitude to my supervisor, Ass.-Prof. Mag. Dr. Verena Pichler. Her constant encouragements and support were vital to guide me to achieving this degree. I have been very fortunate to have had the opportunity of working with such a dedicated mentor, and I will always be more than thankful for everything I have been able to learn from her along the way.

Secondly, I would like to express my gratitude towards the department of pharmaceutical science, especially the Pichler Group. I'm grateful for the encouraging environment created by the group, the support and helpful guidance will always be highly appreciated. Furthermore, I would like to thank Sarah Stellnberger and Lukas Kogler for the ^{1}H-NMR measurements during my experimental work.

Additionally, I am very thankful for my supportive family all throughout my studies, their encouragement and financial support were essential in my journey of pursuing my academic career. I will always be deeply grateful.

Lastly, I would like to thank my friends and fellow students for the constant support and positive energy. Their moral support and academic guidance have significantly contributed to me overcoming various obstacles during this time, which will forever be greatly appreciated.

Zusammenfassung

Die Positronen-Emissions-Tomographie (PET) ist ein nicht-invasives Diagnosetool in der medizinischen Bildgebung, das in einem erheblichen Maße von der Verfügbarkeit und Selektivität radioaktiv markierter Substanzen abhängt. Vorstufen und prosthetische Gruppen sind eine entscheidende Komponente bei ihrer Synthese, da sie die für die radioaktive Markierung erforderlichen Funktionalitäten bereitstellen.

Ziel dieser Arbeit war es, eine Synthesestrategie für eine niedermolekulare Verbindung und einen bioorthogonalen Linker zu entwickeln, die speziell für die Fluor-18-Markierung geeignet sind. Die dreistufige Synthese von 3-[2-(4-Fluorbenzyl)imidazo[2,1-b][1,3]thiazol-6-yl]-2H-Chromen-2-on erforderte zunächst die Bildung eines Diazoniumsalzes und anschließend dessen Reaktion mit Acroleindiethylacetal. Es wurden verschiedene Reaktionsbedingungen wie Temperatur und pH-Wert getestet.

Der Fokus wurde dann auf die Synthese des Linkers unter Verwendung einer Bicyclo[6.1.0]non-4-yne (BCN)-Verbindung gelegt, die für eine anschließende Click-Reaktion mit 5'-C3-Azid vorgesehen war. Es wurden Experimente durchgeführt, um die Reaktivität der Verbindungen und die Bedeutung der Basenauswahl zur Verbesserung des Syntheseergebnisses zu untersuchen. Nach Anpassungen der Syntheseroute durch Hinzufügen der BOC-Gruppe am Amin von Ethanolamin lieferte die dritte Syntheseroute vielversprechende Ergebnisse für den ersten und zweiten Schritt der 4-stufigen Synthese und legte damit den Grundstein für künftige Verfeinerungen.

Die Ergebnisse dieser Arbeit bieten eine solide Grundlage für die weitere Optimierung der Synthesen und tragen zur ständigen Weiterentwicklung der molekularen Bildgebung im biomedizinischen Bereich bei.

Abstract

Positron emission tomography (PET) imaging is a non-invasive diagnostic tool in medical imaging, relying heavily on the availability and selectivity of radiolabelled compounds. Precursors and prosthetic groups serve as a crucial component in their synthesis, as they provide the necessary functionalities required for radioactive labelling.

This work aimed to establish a synthesis strategy for a small molecule and a bioorthogonal linker, specifically tailored for fluorine-18 labelling. First, the 3-step synthesis of 3-[2-(4-fluorobenzyl)imidazo[2,1-b][1,3]thiazol-6-yl]-2H-chromen-2-one required the formation of a diazonium salt followed by its reaction with acrolein diethyl acetal. Different diazotization agents and reaction conditions such as temperature settings and pH-levels were tested.

The focus was then shifted to the synthesis of the crosslinker molecule utilizing a bicyclo[6.1.0]non-4-yne (BCN) compound, intended for a subsequent click reaction with 5'-C3-azide. Experiments were conducted to examine the reactivity of the compounds and the importance of the base selection to improve the outcome of the synthesis. Following adjustments of the synthesis route by protecting the amine end of ethanolamine with a BOC (tert-butyloxycarbonyl)-protecting group, the third synthesis plan provided promising results for the first and second step of the 4-step synthesis, setting the groundwork for future refinement.

The outcomes of this research offer a solid foundation for further optimization of the small molecule syntheses, contributing to the constant evolution in the development of molecular imaging tools in the biomedical field.

Table of Contents

1. Introduction

Radiopharmaceuticals are radioisotopes with the purpose of targeting specific biological functions within the human body. When approved, these radioactive drugs are used for diagnostic purposes, e.g. by positron emission tomography (PET), and increasingly for the therapy of a variety of diseases. First, a precursor molecule is required, which then undergoes a labelling process with a suitable radioactive organic isotope of choice. The radioactive compound is set to target a certain biological function with the highest possible specificity. In this work, the respective target is the Midkine (MDK) growth factor, which will be discussed further in the following section.

1.1. Midkine growth factor

MDK is a heparin-binding cytokine and a growth factor that plays a substantial role in several physiological and pathological processes. MDK is involved in cell growth, survival, migration, and angiogenesis, resulting in being a key factor in the development and repair of tissue. Furthermore, it is involved in inflammatory reactions and often overexpressed in various cancers, including breast, lung and prostate cancer, making it a potential target for a selection of cancer studies. Also, MDK inhibitors are expected to be useful in the treatment of rheumatoid arthritis, multiple sclerosis, hypertension and renal diseases.[1,2] MDK is a soluble cytokine, which means that if its levels are elevated, it can be detected in bodily fluids such as blood, urine, and cerebrospinal fluid. This makes MDK a convenient and non-invasive biomarker for early disease detection and screening.[3,4]

Radiolabelled compounds targeting MDK can be utilized for non-invasive diagnostic imaging. These imaging agents allow for the visualization and localization of MDK expression in tumours using PET or single-photon emission computed tomography (SPECT). To minimize off-target adverse pharmacological effects in humans, it is essential to achieve high specific radioactivity in radiopharmaceutical preparations for effective tumour imaging.[5,7]

Radiolabelled compounds can also be explored for therapeutic purposes, as they can deliver specifically targeted radiation to MDK-overexpressing cancer cells, potentially inhibiting their growth or inducing apoptosis. Targeting MDK with radiotherapeutic agents holds promise as a targeted cancer treatment strategy, especially in cases where MDK is involved in cancer progression.[5–7]

1.2. PET Imaging

PET is an imaging technique predominantly utilized in clinical routine and research to diagnose and identify biological processes in vivo. PET is increasingly used in clinical neurology and oncology, allowing a deeper insight into disease pathogenesis and progression, further broadening the spectrum of monitoring patient response to treatment. PET paves the way for in vivo examinations of cerebral function, hemodynamics, metabolic processes and receptor affinities, among others, thus contributing to an extensive understanding of physiological intricacies. The non-invasive nature of PET involves the administration of a radiotracer via intravenous injection.[8]

PET utilises the fact that electrons and positrons have identical mass but opposite charge, and being antiparticles, cannot coexist together. During positron emission, a proton decays into a neutron, in the case of ^{18}F specifically, it decays to ^{18}O. The nucleus emits a neutrino (ν) and a positron (β^+), as described in Figure 1. The kinetic energy of the positron is released within a short distance of the decay site, and the particle subsequently collides with an electron, resulting in an annihilation event. The emission of energy produces two gamma rays, which are scattered in precisely the opposite direction (180°). The PET scanner is composed of a circular array of scintillation counters. An event is registered only when the two emitted gamma rays are detected almost simultaneously. The resulting signals are digitized and processed by a computer, which then reconstructs the activity distribution and visualizes it.[9–11]

$$^{18}F \longrightarrow {}^{18}O + \beta^+ + \nu$$

Figure 1: Radioactive decay of the radioisotope fluorine-18[9]

The radioisotope of choice requires to be readily accessible and with a long enough half-life to ensure safe distribution efforts, yet short enough to ultimately reduce the radiation exposure for the patient.[10] Accordingly, PET radiopharmaceuticals such as ^{11}C, ^{13}N, and ^{18}F are produced using a cyclotron through irradiation of ^{14}N, ^{16}O, and ^{18}O, as presented in Figure 2. Cyclotrons produce positron-emitting radionuclides by bombarding a specific target with charged particles that are accelerated in the process.[9] The biological compound of interest is labelled with a positron emitting isotope, preferably fluorine-18 (^{18}F). It is one of the most widely used due to its unique combination of long half-life, clean decay profile (97% positron emission and 3% electron capture) and low positron energy, resulting in high resolution PET images.[10,12,13]

	O-15	N-13	C-11	F-18
half-life	2 min	11 min	20 min	110 min
availability	on-site cyclotron	on-site cyclotron	on-site cyclotron	cyclotron, regional distribution

Figure 2: Positron-emitting organic isotopes of interest in PET imaging[10]

The glucose analogue 2-[^{18}F]FDG (2-[^{18}F]fluoro-2-deoxy-D-glucose) is one of the most popular PET tracers and is used to image glucose uptake, as shown in Figure 3. 2-[^{18}F]FDG is transported via glucose transporters and phosphorylated within the cell, resulting in [^{18}F]FDG-6-phosphalate being trapped and accumulating. This event is based on the presence of the ^{18}F atom which prohibits the integration of [^{18}F]FDG-6-phosphalate into the glycolytic pathway. 2-[^{18}F]FDG has numerous applications in cardiology, neurology, and oncology.[10–14]

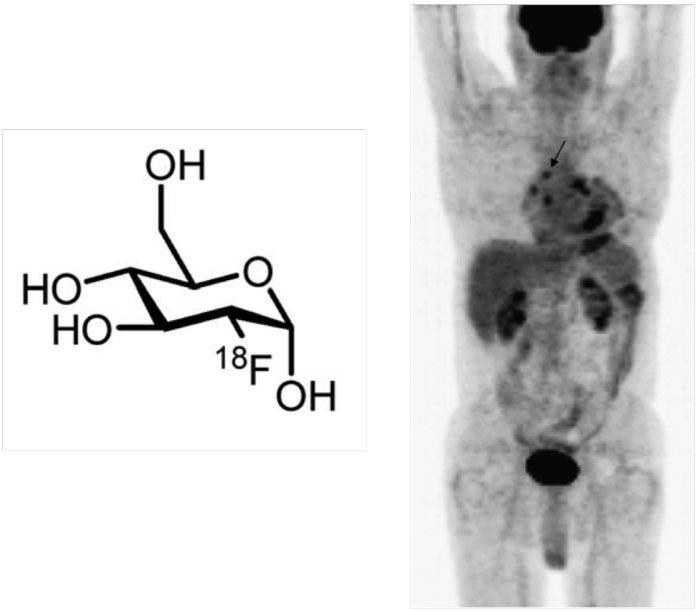

Figure 3: Structure of 2-[^{18}F]FDG[15]; PET imaging with 2-[^{18}F]FDG in patient with small cell lung cancer showing multiple mediastinal lymph nodes with -[^{18}F]FDG activity[16]

To trace a biological function, PET requires the presence of a radiotracer. Therefore, numerous radiotracers must be developed to cover the respective biological functions of interest. The radiolabelling strategy is a crucial step to ensure highly reproducible and efficient labelling with the respective positron-emitting radioisotope. The following section gives an overview of a selection of commonly utilized radiolabelling strategies.

1.3. Labelling Strategies for Fluorine-18

The two chemical synthetic routes predominantly utilized to directly incorporate fluorine-18 (^{18}F) into a precursor compound generally fall into two categories: electrophilic and nucleophilic reactions. These approaches introduce ^{18}F in the molecule of interest in a single step. Two different sources for the ^{18}F come into operation, the first being molecular [^{18}F]fluorine [^{18}F]F_2 (electrophilic) and the second [^{18}F]fluoride (nucleophilic). Incorporating ^{18}F in bioactive molecules can also be realized with the use of prosthetic groups (PG) to overcome obstacles in the process, when compounds are not well suited for direct fluorination.[9]

1.3.1. Electrophilic fluorination

Electrophilic fluorination is an established reaction in which ^{18}F is introduced into electron-donating reactants to form a carbon-fluorine covalent bond, as described in Figure 4. An often facilitated reagent for this procedure is [^{18}F]F_2. The most common approach to produce [^{18}F]F_2-gas involves the $^{20}Ne(d,\alpha)^{18}F$ nuclear reaction, which is a carrier-added method. A small amount of fluorine-19 gas is necessary to enable the recovery of the radioisotope. However, this technique leads to low specific activity due to the excessive presence of F_2 molecules. Recoveries from this system range from 50-70% based on several conditions in addition to losses by the lack of stereospecificity of the available [^{18}F]F_2 reagent.

An alternative method involves the $^{18}O(p,n)^{18}F$ nuclear reaction by employing O_2 gas to create fluorine ([^{18}F]F_2). While the "double shoot" method can produce several GBq levels of [^{18}F]F_2, it suffers from low specific activity and is complex. This method involves sequential irradiations with an inert gas:F_2 mixture and [^{18}O]O_2. Additionally, the target used for [^{18}F]F_2 requires a deuteron beam of such great energy often not available on hospital cyclotrons.[17–21]

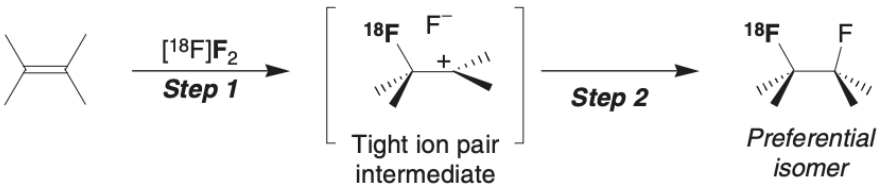

Figure 4: Mechanism of electrophilic fluorination of a carbon-carbon double bond[17]

1.3.2. Nucleophilic fluorination

Nucleophilic ^{18}F-fluorination is reportedly more attractive than electrophilic ^{18}F-fluorination, considering its convenience and reliability in terms of radioisotope production. The current approach to produce [^{18}F]fluoride utilizes a no-carrier-added method. It involves the nuclear reaction of ^{18}O(p,n)^{18}F using ^{18}O-enriched water target. The resulting [^{18}F]F$^-$ lacks nucleophilicity due to solvation, requiring elaborate preparation steps to enhance effectiveness, such as azeotropic drying steps.

To maintain high specific activity in the final product for PET imaging, careful chemical approaches, material selection, and handling are crucial. Fluorination can be applied to both aliphatic (S_N2) and aromatic compounds (S_NAr). The reaction mechanism is visualized in Figure 5. The optimal precursors for SNAr reactions with [^{18}F]fluoride usually requires a leaving group, common groups being Br, I, Cl, and sulphonyl esters (triflate, mesylate or tosylate). The leaving ability varies significantly and decreases as followed: –OTf > –OTs ≈ –OMs > –I > – Br > –Cl. An activating electron-withdrawing group like –NO_2, –CN, –CF_3, or –CO in the ortho or para position helps stabilizing the complex, making SNAr reactions easier. Activation by electron-withdrawing groups is a necessity for S_NAr. Reaction conditions involve polar aprotic solvents (acetonitrile, dimethylformamide, dimethyl sulfoxide) at 80–180°C for 5–30 min. To enhance the solubility and reactivity, nucleophilic fluorinations employ phase transfer catalysts (e.g., Kryptofix 2.2.2) with basic reaction mixtures influencing possible competitive elimination reactions. In several publications, protic solvents like tertiary alcohols have been applied in routine ^{18}F-tracer production via nucleophilic reactions.[14,17–21]

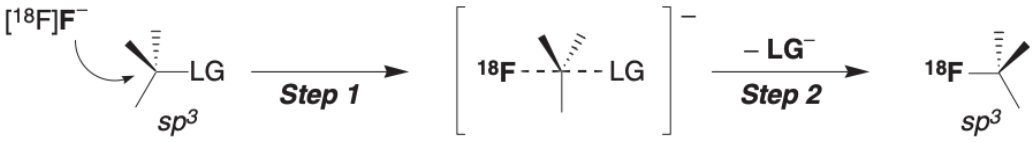

Figure 5: The S_N2 mechanism of nucleophilic aliphatic fluorination[17]

The radiosynthesis of e.g. 2-[^{18}F]FDG, as shown in Figure 6, depicts the most representative example of aliphatic nucleophilic substitution. The prevailing synthesis approach utilizes [^{18}F]fluoride which reacts with the triflate leaving group of the precursor in the presence of a catalyst. Acetyl groups serve as protecting groups for the remaining hydroxyl groups, subsequently removed by base-catalysed hydrolysis, e.g. yielding 2-[^{18}F]FDG up to 80%. Nowadays, the synthesis is fully automated, allowing high yields, increasing reproducibility and simplifying distribution.[12,20]

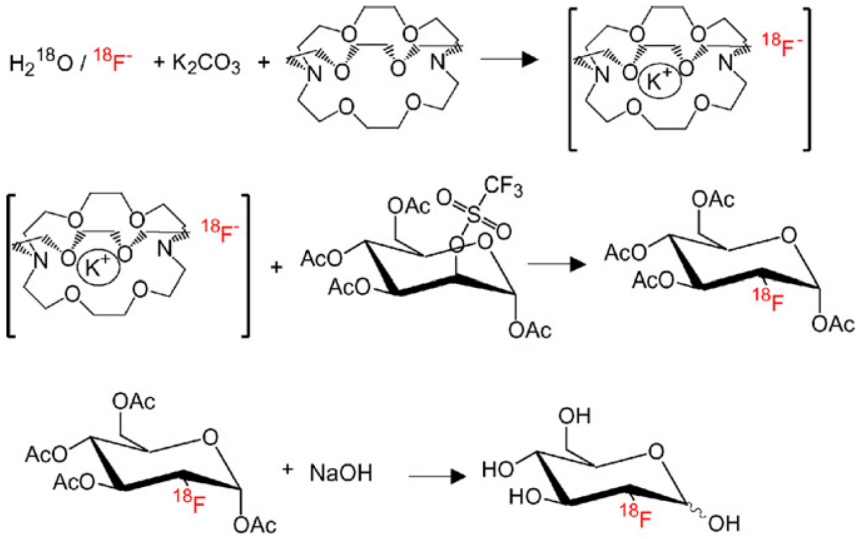

Figure 6: Radiosynthesis of 2-[^{18}F]FDG via nucleophilic substitution[15]

1.3.3. Prosthetic Groups for Fluorine-18 Labelling

Rather than employing fluoride directly, an alternative approach involves PG labelling, wherein a small, functionalized no-carrier-added group is added to a target molecule of higher molecular weight. Such target molecules may include nucleotides, peptides, and proteins. PGs are a tool to overcome the inability to radiolabel certain compounds with ^{18}F via nucleophilic substitution.[21,22] Once synthesized, these synthons can be utilized in all kinds of different molecules by the common chemical reactions:

I. Alkylation: Analogous to [^{11}C] methylations, this method involves adding alkyl groups onto phenols, amines, or thiols. Prominent synthons within this category include [^{18}F]fluoromethyl, ethyl, propyl, or benzyl halide, as well as sulphonyl esters.

II. Amide bond formation: This technique finds application in peptide labelling, employing activated esters such as N-hydroxy-succinimidyl-[^{18}F]fluorobenzoic acid (SFB).

III. Acylation: Developed as a strategy for labelling alcohols and amines with ^{18}F at no-carrier-added levels, this technique typically employs 2-[^{18}F]fluoropropionic acid methyl ester. Optimization for large biologically active molecules containing $-NH_2$ groups may necessitate an additional step, incorporating base and dicyclohexyl carbodiimide, to convert the ester to its free acid form. However, it is comparatively less efficient than the utilization of SFB.[18,23]

[^{18}F]SFB

^{18}F-active esters, shown in Figure 7 (B), were introduced as PGs to allow for labelling of larger biomolecules like peptides and proteins under mild aqueous conditions, as direct ^{18}F-labeling approaches were not available at the time. The most notable example of an active ester PG is N-succinimidyl-4-[^{18}F]fluorobenzoate ([^{18}F]SFB introduced by Vaidyanathan and Zalutsky and helped set off significant research efforts to develop new and more efficient active ester PGs.[24] The initial multi-step synthesis of [^{18}F]SFB has undergone several modifications to improve its convenience for routine use. However, it still takes around one to two hours to synthesize. Other esters like tert-butyl esters and sulfonated PGs have been introduced to address various limitations of [^{18}F]SFB like synthesis time and properties of the transferred group.[22,25]

[^{18}F]FETos

2-[^{18}F]fluoroethyl tosylate, as seen in Figure 7 (A), was first introduced by Block and Coenen and became one of the most widely used fluorine-18 prosthetic groups (PG) for radiolabelling.[14] It functions as an ^{18}F substitute for carbon-11 methyl iodide, allowing easier synthesis and distribution of tracers compared to short-lived carbon-11. The synthesis of [^{18}F]FETos is very reliable, efficiently yielding the PG in up to 82% radiochemical yield. [^{18}F]FETos exhibits a good balance of reactivity and stability, making it an ideal candidate for reacting with nucleophilic groups such as amines and alcohols over a wide pH range. It is widely used for radiolabelling small organic molecules, peptides, and other compounds under 1000 Da. However, it is less suited for larger molecules like proteins due to lower reactivity. Despite structural differences from carbon-11 tracers, [^{18}F]FETos allowed evaluation of many potential radiotracers and established fluorine-18 PG chemistry.[22,26]

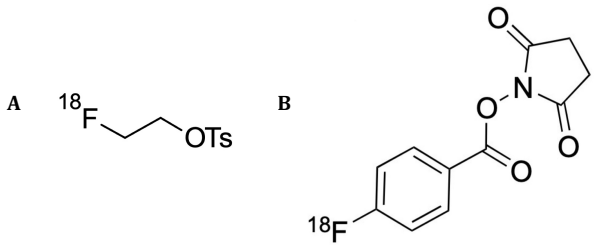

Figure 7: Structure of [^{18}F]FETos (A)[26] and [^{18}F]SFB (B)[27]

Click Chemistry

Click chemistry reactions gained widespread use in radiolabelling due to their specificity and mild reaction conditions. There are three commonly utilized reactions with a key distinction lying in the catalysis requirement and bioorthogonality. The term click chemistry defines several reactions that are characterized by short reaction times, relatively simple procedures and high yields. Click reactions can proceed selectively in biological systems without interfering with other biochemical processes or endogenous functional groups.[28] The most common reaction types for click chemistry are the Diels Alder reaction, Huisgen cycloaddition and the developed variant using strain-promoted alkynes, which will be discussed in detail.

The Inverse-Electron Demand Diels-Alder (IEDDA) reaction follows a [4+2] cycloaddition between a dienophile (strained alkene or alkyne) and a diene (tetrazine). The strain-promoted version of IEDDA is catalyst-free, although metal-catalysed versions exist. Furthermore, the biorthogonality allows selective reactions in biological systems, but metal-catalysed versions may raise concerns regarding biological applications.[23,28–30]

The Huisgen cycloaddition reaction involves the 1,3-dipolar cycloaddition between an azide and an alkyne forming a triazole ring, as described in Figure 8 (A). This process needs a copper(I) catalyst to accelerate the reaction, yet the presence of copper can sometimes be a concern in biological applications due to potential toxicity. Although efficient, the reaction rate may be affected by the concentration of reactants and the copper catalyst, leading to compatibility problems with biological systems.[9,28]

In order to overcome the limitations of the Huisgen cycloaddition, Bertozzi et al. developed the Strain-Promoted Alkyne Azide Cycloaddition (SPAAC). In contrast, SPAAC does not rely on a copper catalyst. It takes advantage of the inherent strain in cyclooctynes, which undergo a faster reaction with azides without additional catalysis, as seen in Figure 8 (B). SPAAC is bioorthogonal, meaning it can occur alongside biological functional groups and is non-interacting (orthogonal) with their functionality. This reaction is straightforward and less prone to issues related to the presence of catalytic species in biological systems. Even at lower concentrations, SPAAC exhibits rapid kinetics, making it suitable for bioconjugation under physiological conditions.[28,30,31]

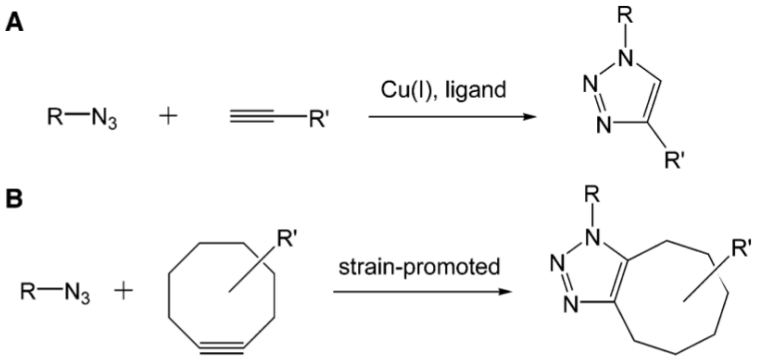

Figure 8: (A) Cu(I)-catalyzed Huisgen cycloaddition; (B) Strain-promoted cycloaddition of azides and cyclooctynes[32]

In the development of the PET radiopharmaceutical, the prosthetic group [^{18}F]BCN is synthesised to label oligonucleotides, among others. Among the variety of cyclooctynes designed for SPAAC reactions, BCN analogues stand out for their minimal synthetic effort. BCN is considered one of the least apolar cyclooctynes, making it applicable for efficient aqueous conjugation reactions. Additionally, BCN compounds have demonstrated rapid cycloadditions, not only with azides but also through IEDDA reactions.[29,33] The activated sulfonate ester is prepared and subjected to ^{18}F-fluorination reactions using established protocols. [^{18}F]BCN is produced in the presence of K[^{18}F]-Kryptofix 2.2.2 (K222) under specified conditions. For example, [^{18}F]BCN was applied for specifically labelling the 5'-C3 azide DNA oligonucleotide 5'-g*a*aaccc5cgccgc5atcct*t*g (Fig. 9,10).[29]

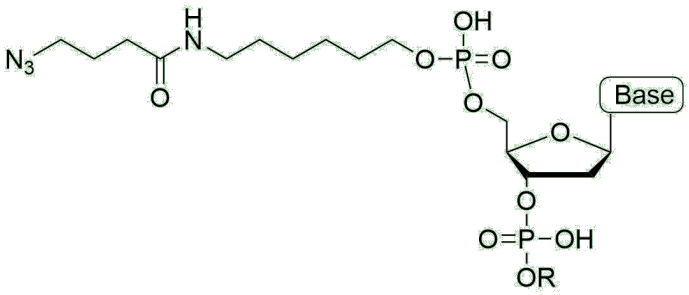

Figure 9: Structure of the 5'-C3 azide DNA oligonucleotide 5'-g*a*aaccc5cgccgc5atcct*t*g[34]

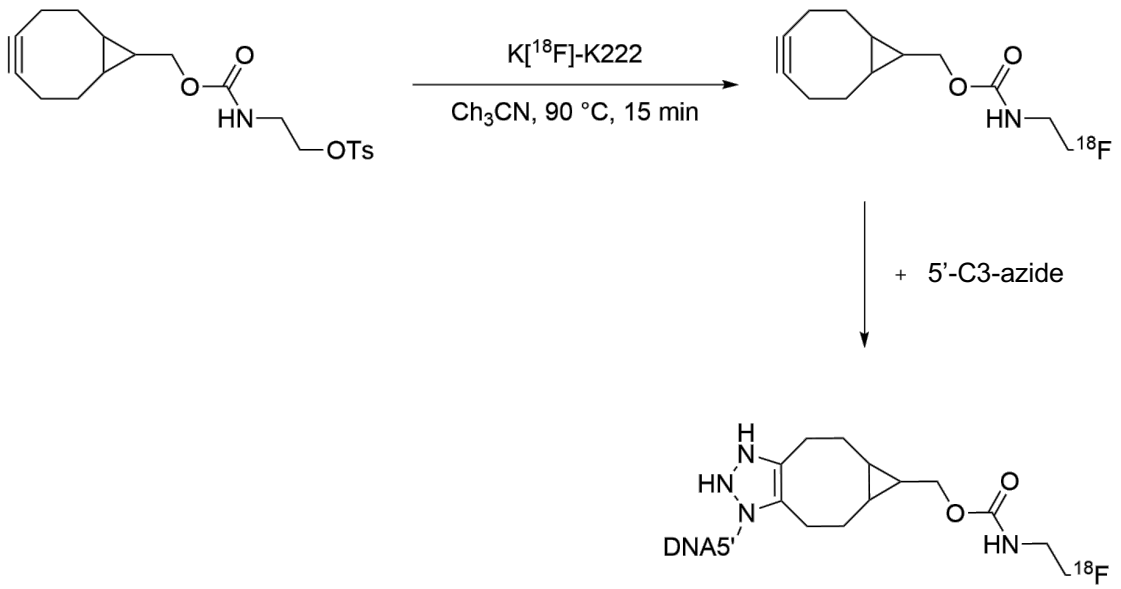

Figure 10: [^{18}F]BCN synthesis procedure and introduction of the PG to the 5'-C3 azide via SPAAC reaction[29]

In order to execute labelling procedures, the first step is to synthesize the required small molecule compounds. Consequently, the following sections explain the theoretical background of chemical reactions applied specifically in this work to achieve the synthesis of a small molecule precursor and a prosthetic group.

1.4. Synthesis of the small molecule 3-[2-(4-fluorobenzyl)imidazo[2,1-b][1,3]thiazol-6-yl]-2H-chromen-2-one

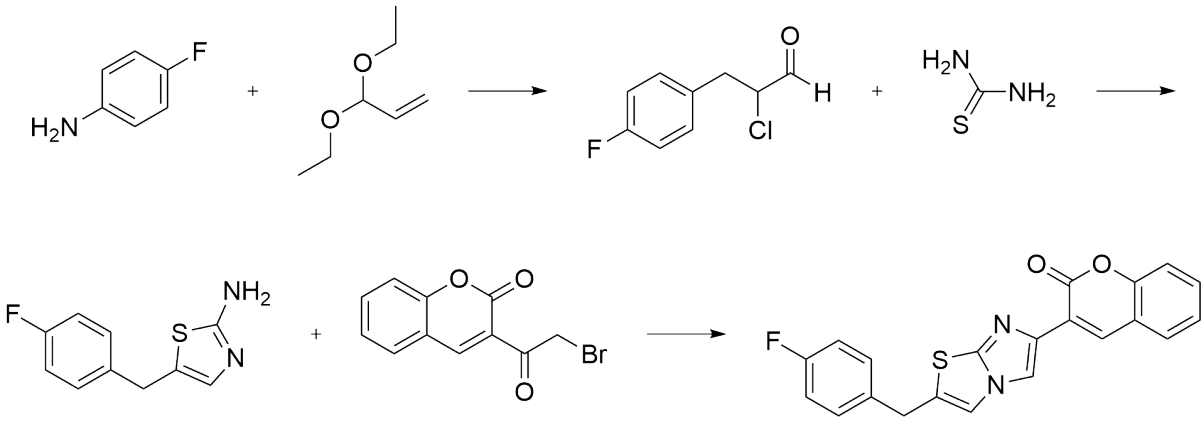

Figure 11: General procedure for the synthesis of 3-[2-(4-fluorobenzyl)imidazo[2,1-b][1,3]thiazol-6-yl]-2H-chromen-2-one

The synthesis of the small molecule follows a route of four steps provided by Prof. Dr. Pichler, presented in Figure 11. The preliminary stage of 2-amino-5-benzyl-2,3-thiazole is obtained by first transforming 4-fluoraniline into diazonium salts directly followed by a reaction with acrolein diethyl acetal to yield 3-aryl-2-chloropropanal with the elimination of nitrogen. The organic chemical reactions employed in the experiments are explained in greater detail in the following subsections. The following ring closure is achieved by introducing thiourea. The reaction with a coumarin-attached halo-aldehyde further leads to the cyclocondensation reaction building the ultimate structure of the precursor.

1.4.1. Diazotization reaction

In the first step of the synthesis, the preparation of a diazonium salt from 4-fluoraniline is required. The diazotization reaction is commonly used in organic chemistry for coupling reactions with aromatic compounds to form azo dyes or other functionalized products. It involves the conversion of a primary aromatic amine to a highly reactive and versatile diazonium salt. The generation of nitrous acid (HNO_2) immediately prior to starting the reaction, depicted in Figure 12, is a key step in the process of diazotization, as the acid decomposes rapidly at room temperature. It is generated by the reaction of sodium nitrite ($NaNO_2$) with a strong mineral acid, typically HCl.[35,36]

Figure 12: Generation of nitrous acid (HNO_2) by $NaNO_2$ and HCl[35]

The nitrogen atoms of the amine and HNO_2 are linked in a first step of the diazotization during the nucleophilic attack of the primary amine targeting the nitrosonium ion, followed by a deprotonation. The protonation of the nitrogen atom of the formed nitrosamine and subsequently the elimination of the water leads to the aromatic diazonium ion, as seen in Figure 13. The diazotization reaction is known for being very sensitive to temperature and pH levels. It is commonly carried out at low temperatures around 0-5 °C to control the reaction and prevent the formation of undesired side products. It is recommended to use 2.5 – 3 equivalents of the acid per mol amine and sodium nitrite in an aqueous solution. As a side product, nitrogen gas is expected to originate from the reaction. To maintain the stability of the nitrous acid and elevate the formation of the diazonium ion, the reaction is typically performed under acidic conditions. Diazonium salt solutions are moderately stable and can therefore only be stored for a short period of time at around 0 °C.[35,36]

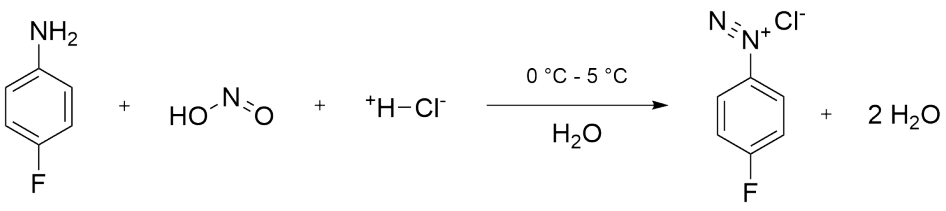

Figure 13: Reaction scheme of the diazotization of 4-fluoraniline

1.4.2. Meerwein reaction

To yield 3-aryl-2-chloropropanal, the subsequent reaction of aryldiazonium salts and acrolein diethyl acetal utilizes the Meerwein arylation. The process typically involves the generation of aryl radicals from aryldiazonium salts in the presence of a copper catalyst. The aryl radicals further react with olefins to form carbon-carbon bonds, leading to the arylation of the olefins, as described in Figure 14.[37,38]

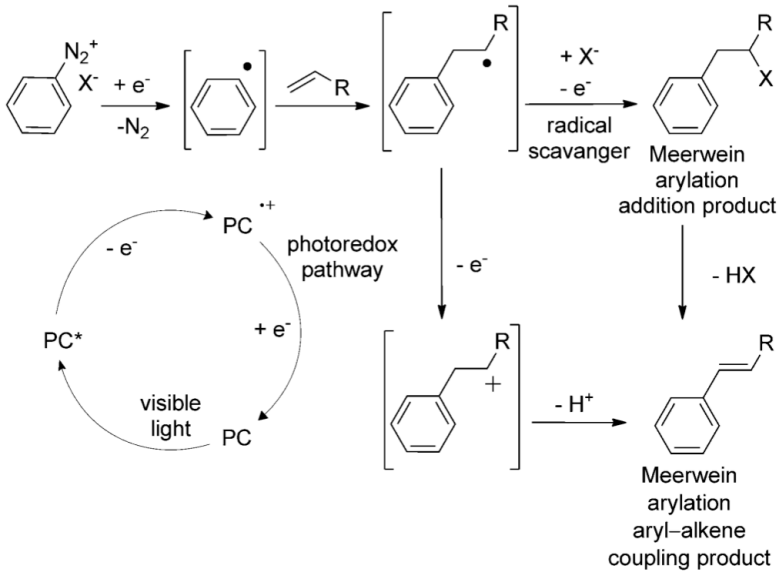

Figure 14: Reaction pathways of the Meerwein arylation addition, cross coupling and photoredox reactions[38]

1.5. First synthesis of the crosslinker 2-(9-bicyclo[6.1.0]non-4-ynylmethoxycarbonylamino)ethyl 4-methyl-benzenesulfonate

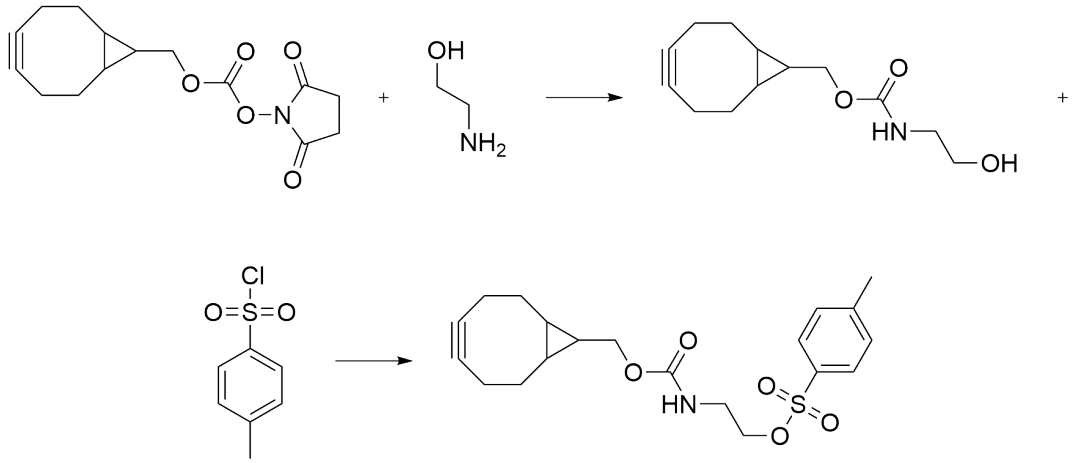

Figure 15: General procedure for the synthesis of 2-(9-bicyclo[6.1.0]non-4-ynylmethoxycarbonylamino)ethyl 4-methyl-benzenesulfonate

The retrosynthesis route for the linker molecule was determined using the AI software IBM RXN for chemistry.[39] The search for a synthesis route yielded limited results, but the chosen approach was anticipated to have the highest confidence in terms of yield. The reaction of (1R,8S,9s)-bicyclo[6.1.0]non-4-in-9-ylmethyl]-N-succinimidylcarbonate with ethanolamine leads to the formation of the 9-bicyclo[6.1.0]non-4-ynylmethyl N-(2-hydroxyethyl)carbamate, as illustrated above in Figure 15. Subsequent tosylation with p-toluenesulfonyl chloride (p-TsCl) under basic conditions completes the synthesis, resulting in the formation of the BCN compound. The organic chemical reactions used in this synthesis route are explained in detail in the following subsections.

1.6. Nucleophilic substitution reaction (S_N1/S_N2)

S_N1 (Substitution Nucleophilic Unimolecular) and S_N2 (Substitution Nucleophilic Bimolecular) reactions are two kinds of substitution reactions wherein a nucleophile (Nu) replaces a leaving group X attached to a carbon atom. The nucleophile attacks the partially electropositive carbon and thereby releases X, as seen in Figure 16. S_N1 and S_N2 differ in their reaction mechanism, stereochemistry and kinetics. The nucleophilic attack of Nu and the nucleofuge exit of X can occur simultaneously in one (S_N2) or successively in two steps (S_N1).[35,36,40]

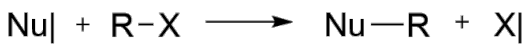

Figure 16: Nucleophilic substitution reaction[36]

S_N1 reaction

S_N1 reactions occur in two consecutive steps. First, X is removed, generating a carbenium ion intermediate which rapidly reacts with the nucleophile Nu, resulting in the final product, shown in Figure 17. Solely the substrate RX participates in the rate-determining step, as S_N1 reactions are first-order, meaning the rate is mainly determined by the concentration of the substrate. The intermediate is high in energy, allowing nucleophilic attack resulting in the formation of racemic mixtures and by-products, e.g. olefines and rearranged compounds. The carbenium ion intermediate is planar, meaning Nu can attack from both sides, which can lead to the formation of two different enantiomers. This type of reaction commonly requires substantial stability of the carbenium ion, such as tertiary substrates.[35,36,40]

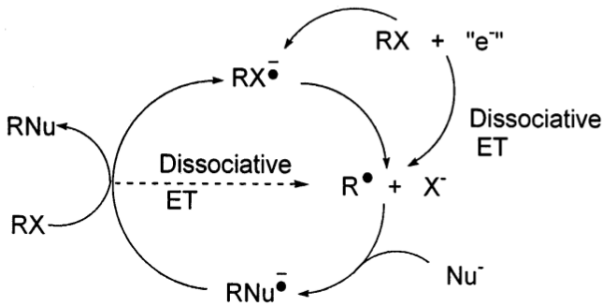

Figure 17: Reaction mechanism S_N1 reaction[40]

S_N2 reaction

S_N2 reactions proceed in a joint single step. The nucleophile attacks the substrate while X departs simultaneously, resulting in the formation of the product without intermediates. Nu approaches RX from the opposite side of the substrate X and promptly interacts with R. The bond gap between

R-X expands while the R-Nu binding occurs. This transitional state is the energetically highest level during the process. S_N2 reactions are second order reactions, thus the rate depends on the concentration of both the substrate and the nucleophile. The transitional intermediate presents five bonds, which allows the Nu to attack from the opposite side of X. This leads to the formation of a single product and can further cause a conversion of configuration at the reaction centre. Also, larger groups around the centre of the reaction obstruct the nucleophilic attack, therefore S_N2 reactions are favoured with primary substrates.[35,36,40]

1.6.1. Tosylation reaction

Aryl tosylates (and mesylates) are frequently utilized as alternatives to aryl halides, as they make good leaving groups due to their chemical and physical properties. Apart from the reduced halide waste, their availability and appropriate reactivity set them apart from other leaving groups, especially alcohols. Despite the preparation from tosylates taking place in comparably mild conditions, there is a selection of potential disadvantages, e.g. long reaction times, higher temperatures, low reactivity for phenols with electron-withdrawing groups and the demand of specific equipment or reagents. A variety of methods is available for the preparation of tosylates. The products often require purification via column chromatography or recrystallization, as by-products are often formed in the process.[41–43] The synthesis approach in this work is shown in Figure 18 and involves the tosylation of the hydroxyl group with p-TsCl in the presence of a sterically hindered amine base (e.g. pyridine or triethylamine) in an anhydrous organic solvent.

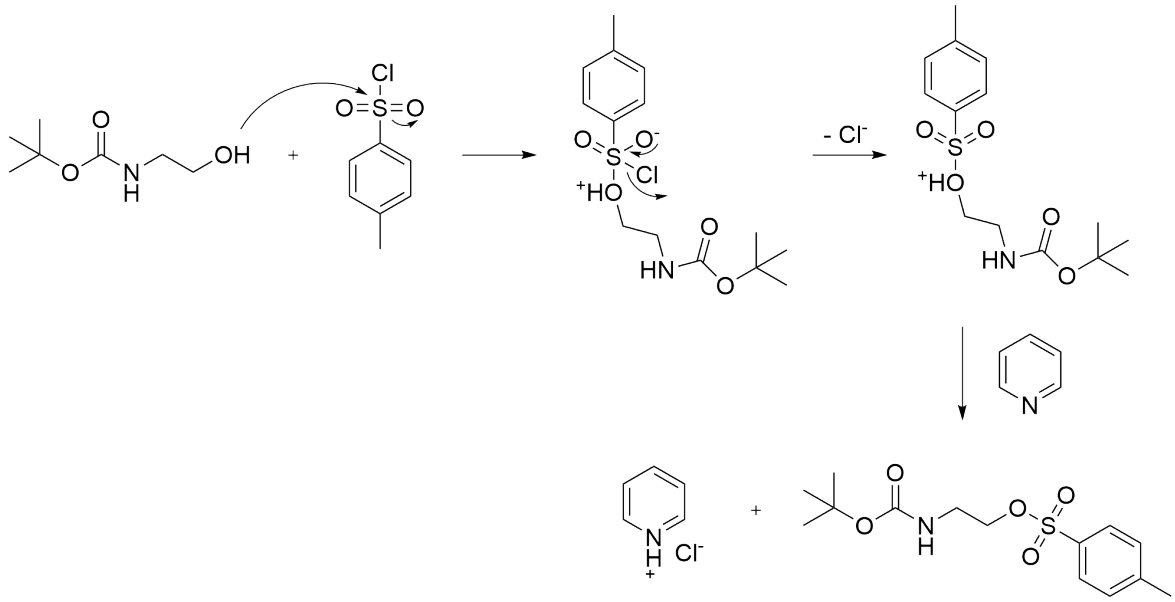

Figure 18: Underlying mechanism of the tosylation reaction and formation of by-product

1.7. Second synthesis of the crosslinker 2-(9-bicyclo[6.1.0]non-4-ynylmethoxycarbonylamino)ethyl 4-methyl-benzenesulfonate

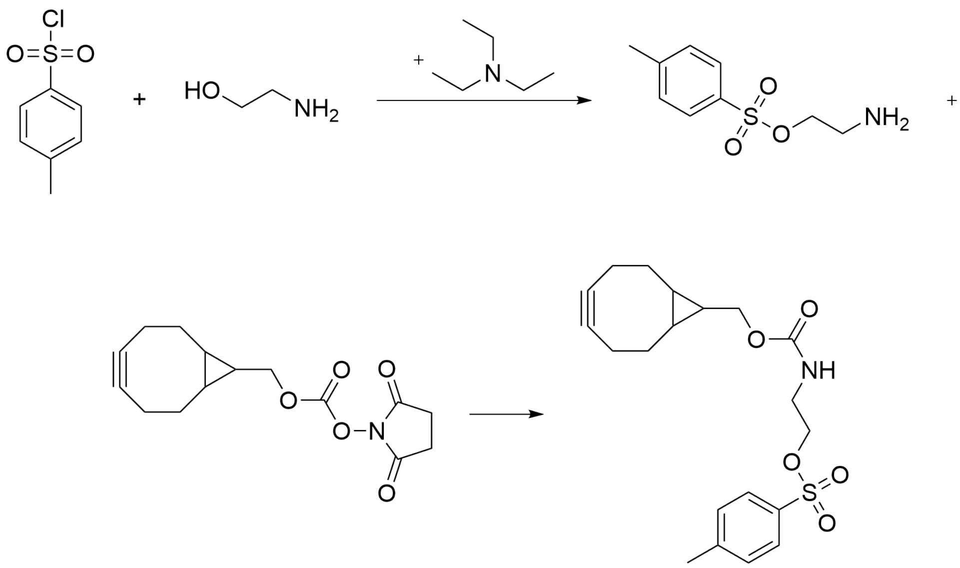

Figure 19: General procedure for the second synthesis of 2-(9-bicyclo[6.1.0]non-4-ynylmethoxycarbonyl-amino)ethyl 4-methyl-benzenesulfonate

The synthesis strategy involves the initial conjugation of ethanolamine with p-TsCl under basic conditions followed by the reaction with the BCN-compound, as shown in Figure 19. This reaction scheme was designed to minimize waste associated with the BCN-compound and mitigate potential stability concerns. This approach facilitated the exploration of various sterically hindered bases for their effectiveness in the reaction. Additionally, experiments could be conducted to examine the reactivity of ethanolamine in relation to the tosylation reaction. The chemical reactions applied in the experiments were identical to those described in the first synthesis route.

1.8. Third synthesis of the crosslinker 2-(9-bicyclo[6.1.0]non-4-ynylmethoxycarbonyl-amino)ethyl-4-methyl-benzenesulfonate

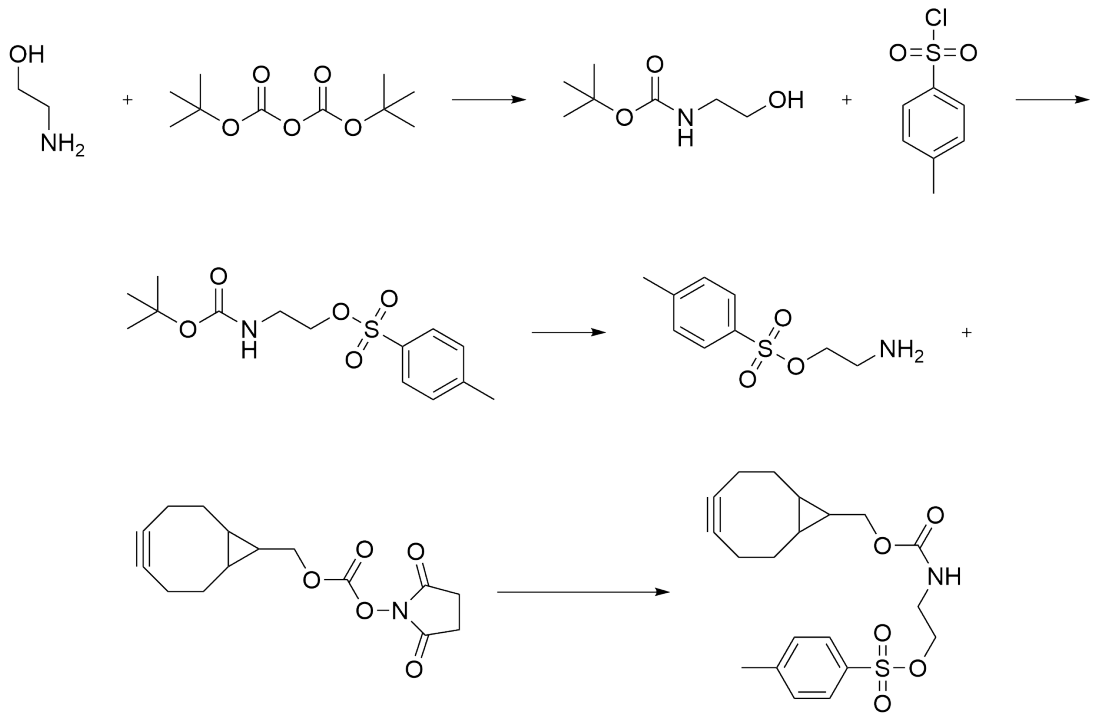

Figure 20: General procedure for the third synthesis of 2-(9-bicyclo[6.1.0]non-4-ynylmethoxycarbonyl-amino)ethyl 4-methyl-benzenesulfonate

This approach involves the protection of the amino group of ethanolamine using Boc_2O, followed by the tosylation reaction specifically targeting the hydroxyl group of ethanolamine, as described in Figure 20. Finally, the removal of the BOC-protecting group is carried out under acidic conditions, such as with trifluoroacetic acid (TFA), preparing the compound for coupling with the BCN-compound through the S_N2 mechanism. The additional BOC-protection is explained in depth in the following subsection.

1.8.1. Protecting groups

In many syntheses, it is necessary to temporarily block functional groups in a molecule to prevent them from participating in the reaction. Protecting groups are used for this purpose, which are introduced into the functional group and removed after the reaction.
The selection of protective groups is based on important criteria:

- Introduction and removal should be performed under mild conditions with minimal loss of yield.
- The necessary reagents for the introduction of the protective group must be easily accessible and have minimum toxicity.
- The protected functional group should remain chemically stable during the intended synthesis conditions.[35,44]

BOC is a commonly used protecting group for amines. It is known to be stable under basic conditions but labile under acidic conditions.[35,45] The N-Boc protected amine is formed by its nucleophilic attack at the carbonyl group, accompanied by the formation of the by-products tert-butanol and carbon dioxide.[46] Due to the CO_2 gas forming during the reaction, it should not be run in a closed system to allow the gas to escape. A base is not essentially required for the reaction, as the second proton from the amine group of the ethanolamine ends up on the by-product tert-butanol. The approach involves the protection of the amino group of ethanolamine using di-tert-butyldicarbonate (Boc_2O) (1:1 molar ratio at room temperature), followed by the tosylation reaction targeting the hydroxyl group of ethanolamine, as shown in Figure 21. Finally, the BOC-protective group is eliminated under acidic conditions e.g. utilizing TFA.[45,47]

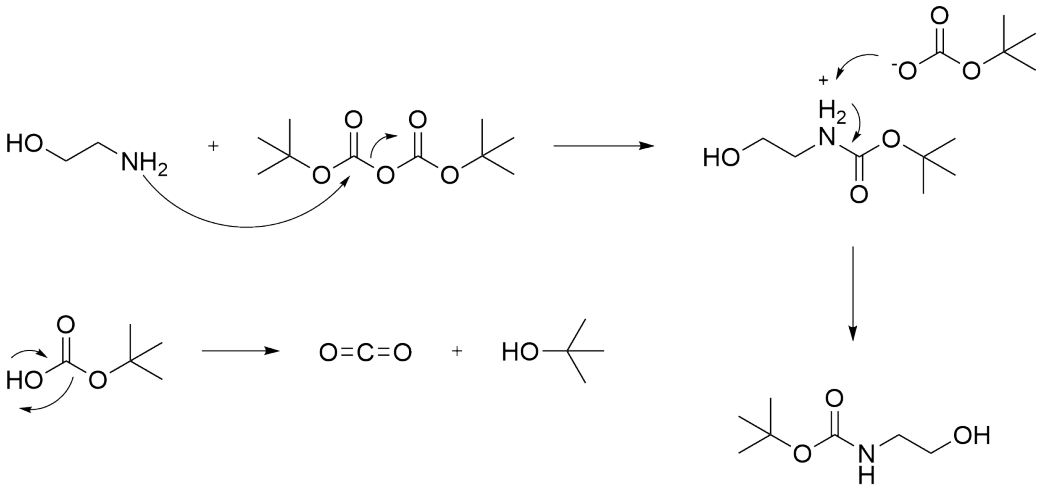

Figure 21: Underlying mechanism N-BOC-protection of ethanolamine; formation of by-products carbon dioxide and tert-butanol[48]

2. Objective

The primary aim of this master thesis was to establish a synthesis strategy for two small molecules. The first small molecule functions as a precursor molecule to inhibit MDK, whereas the second small molecule can be applied as a PG to label a DNA fragment, which again targets MDK. The expected outcome is the generation of two molecules utilized to produce precursors readily available for ^{18}F-labelling.

To achieve the synthesis of the two molecules, the goal of this work was to

1) establish a 3-step-synthesis route for the small molecule iMDK precursor by testing various reaction conditions.
2) establish a 2-step procedure for the PG and optimize the synthesis route by conducting experiments concerning the reactivity of each compound.
3) characterize the intermediates and products of both syntheses by respective analytical procedures such as ^{1}H-NMR, HRMS, IR and TLC measurements.

3. Experimental part

3.1. Materials

3.1.1. Reagents

Table 1: Reagents and solvents

Name of substance (IUPAC)	CAS-number	Origin of material
4-Fluoraniline	371-40-4	Sigma-Aldrich
p-Toluenesulfonic acid	104-15-4	Sigma-Aldrich
Sodium nitrite	7632-00-0	Sigma-Aldrich
Acrolein diethyl acetal	3054-95-3	Sigma-Aldrich
Cupric chloride	7447-39-4	Sigma-Aldrich
Hydrochloric acid	7647-01-0	Sigma-Aldrich
(1R,8S,9s)-Bicyclo[6.1.0]non-4-in-9-ylmethyl]-N-succinimidylcarbonate	1516551-46-4	Sigma-Aldrich
Ethanolamine	141-43-5	Fluka
Pyridine	110-86-1	Sigma-Aldrich
p-Toluenesulfonyl chloride	98-59-9	Sigma-Aldrich
N-N-Diisopropylethylamine	7087-68-5	Sigma-Aldrich
Triethylamine	121-44-8	Sigma-Aldrich
Ammonium chloride	12125-02-9	Sigma-Aldrich
Sodium sulfate, anhydrous	7757-82-6	Alfa Aesar
Sodium chloride	7647-14-5	Sigma-Aldrich
2-propanol	67-63-0	Sigma-Aldrich
Phenylethylamine	64-04-0	Alfa Aesar
Di-tert-butyldicarbonate	24424-99-5	Sigma-Aldrich
Solvents		
Chloroform-d	865-49-6	Sigma-Aldrich
Toluene	108-88-3	Sigma-Aldrich
Hexane	110-54-3	Sigma-Aldrich
Ethyl acetate	141-78-6	Sigma-Aldrich
Dichloromethane	75-09-2	Sigma-Aldrich
Tetrahydrofurane	109-99-9	Sigma-Aldrich

3.1.2. Software

- Mestrenova (Mestrelab Research S.L., Version: 10.0.2-15465)
- ChemDraw (Perkin Elmer, Version: 20.0.0.41 Professional)
- OPUS (Bruker Optik GmbH 2014, Version: 7.5)

3.2. Characterization

3.2.1. Nuclear magnetic resonance (NMR)

^{1}H-NMR spectra were recorded on a 400 MHz Ascend™ Bruker spectrometer and referenced to the solvent $CDCl_3$. The following abbreviations have been used for spin multiplicity: s = singlet; d = duplet; t = triplet; q = quadruplet; m = multiplet; br = broad signal.

3.2.2. Mass spectrometry (MS)

High resolution mass spectra were measured on maXis ESI-Qq-TOF mass spectrometer in DCM (0.1 – 0.5 mg/ml).

3.2.3. Infrared (IR) Spectroscopy

Infrared spectroscopy was performed on Bruker ALPHA FT-IR-Spectrometer and the data was evaluated using Microsoft Excel.

3.2.4. Purification

Purification was carried out on a Biotage® Selekt with different solvent compositions. The stationary phase consisted of Sfar Silica HC D columns of varying sizes (5 g or 10 g).

3.2.5. Thin layer chromatography (TLC)

Thin layer chromatography ALUGRAM Xtra SIL G/UV_{254} DC ready-to-use films from Macherey-Nagel were used with a coating of 0.20 mm silica gel 60 F_{254}, purchased from Thermo Fisher Scientific. A selection of staining reagents was used for detection: saturated aqueous potassium permanganate solution and vanillin reagent (amines, amino acids).

3.3. Synthesis of 3-aryl-2-chloropropanal

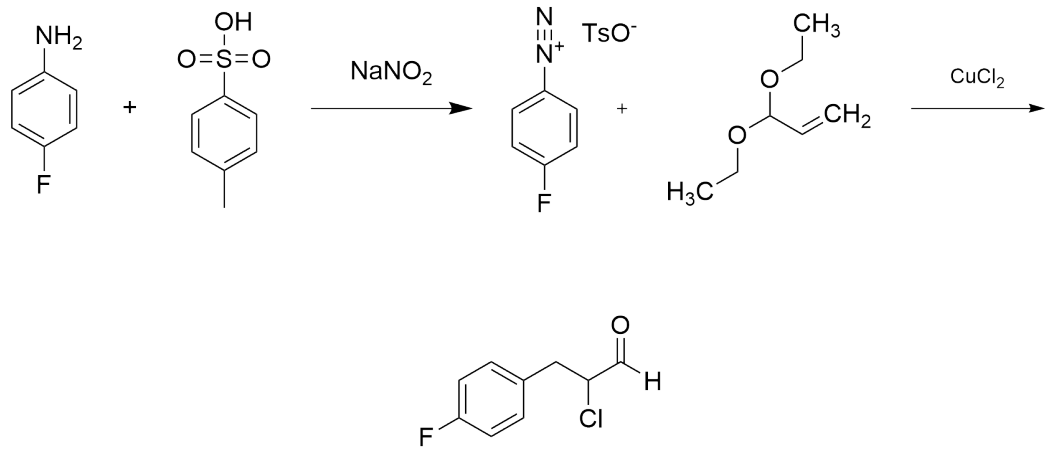

Figure 22: Reaction scheme for the synthesis of 3-aryl-2-chloropropanal

Table 2: Reagents used in the synthesis of 3-aryl-2-chloropropanal

synthesis	substance	M [g/mol]	m [g]	n [mmol]	V [ml]	ρ [g/ml]	equiv.
rola 1+2	**4-fluoroaniline**	111.12	0.100	0.900	0.085	1.173	1.00
	p-TsOH	172.20	1.395	8.099	-	-	9.00
	sodium nitrite	68.99	0.559	8.099	-	-	9.00
	acrolein diethyl acetal	130.18	0.117	0.900	0.140	0.860	1.00
	copper chloride	134.45	0.045	0.335	-	-	0.37

In a two-necked round-bottomed flask equipped with a septum and a cooler, copper chloride ($CuCl_2$) was suspended in 0.5 ml of toluene, as shown in Table 2. Acrolein diethyl acetal was subsequently added. Concurrently, in another round-bottomed flask, p-toluenesulfonic acid (p-TsOH) was dissolved in 8 ml of water. After the addition of 4-fluoroaniline, the compounds were stirred for one minute. Sodium nitrite ($NaNO_2$) was dissolved in 0.5 ml of water and added gradually under rigorous stirring while maintaining the reaction mixture on ice. The resulting cold diazonium salt solution was carefully added drop by drop to the acrolein/$CuCl_2$ suspension. TLC controls were conducted (toluene/EtOH 9:1, hexane/ethyl acetate in different ratios). Following an overnight stirring period, additional toluene was introduced as the organic layer was scarcely visible. The organic phase was separated using a separatory funnel, and the water phase was extracted with ether (3x). The combined organic phases were then dried over Na_2SO_4 and filtered. The product was concentrated under reduced pressure and analysed via ^{1}H-NMR. No product was obtained from this reaction.

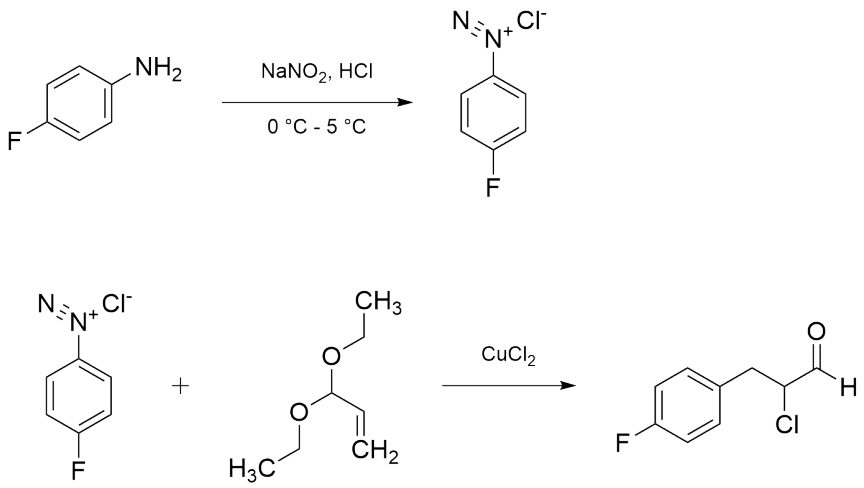

Figure 23: Adjusted reaction scheme for the synthesis of 3-aryl-2-chloropropanal

Table 3: Reagents used in the adjusted synthesis of 3-aryl-2-chloropropanal

synthesis	substance	M [g/mol]	m [g]	n [mmol]	V [ml]	ρ [g/ml]	equiv.
rola 3-10	**4-fluoroaniline**	111.12	0.100	0.900	0.085	1.173	1.00
	6 N HCl	36.46	0.491	2.700	0.450	1.090	3.00
	sodium nitrite	68.99	0.621	0.900	-	-	1.00
	acrolein diethyl acetal	130.18	0.117	0.900	0.140	0.860	1.00
	copper chloride	134.45	0.045	0.333	-	-	0.37

The preparation of the diazonium salt solution was initiated by dissolving 4-fluoraniline in 6 N HCl in a round-bottom flask, as outlined in Table 3. Subsequently, a 2.5N $NaNO_2$ aqueous solution was slowly added dropwise to the stirring mixture while maintaining the reaction on ice. To monitor the progress, iodine starch paper was utilized towards the completion of $NaNO_2$ addition, with the test needing to exhibit positive results (black dots) five minutes later. Concurrently, in another round-bottom flask, a suspension of $CuCl_2$ in toluene was prepared. Following the addition of acrolein diethyl acetal, the cold diazonium salt solution was transferred to this mixture. After three hours of stirring, the toluene phase was collected using a separatory funnel. The water phase was extracted with ether (3x), and the collected organic phases were dried using Na_2SO_4 before being filtered into a pointed flask. The product obtained was concentration under reduced pressure, and measurements involving both ^{1}H-NMR and MS were conducted. Purification of the product rola6 was carried out on Biotage (mobile phase: acetonitrile/methanol 1:4). No product was yielded from this reaction.

The same reaction was repeated with adjustments during the synthesis procedure. First, the diazonium salt solution was neutralized by adding $NaHCO_3$ dropwise to achieve a pH level within the range of 6 to 7 and 0.2 g MgO were introduced to the mixture. In another modified approach, the reaction was carried out at different temperature settings by introducing the diazonium salt

to the acrolein/$CuCl_2$ suspension maintained at 60, 70, and 80 °C. Both attempts of reactions did not yield product.

3.4. Synthesis of 9-bicyclo[6.1.0]non-4-ynylmethyl N-(2-hydroxyethyl)carbamate

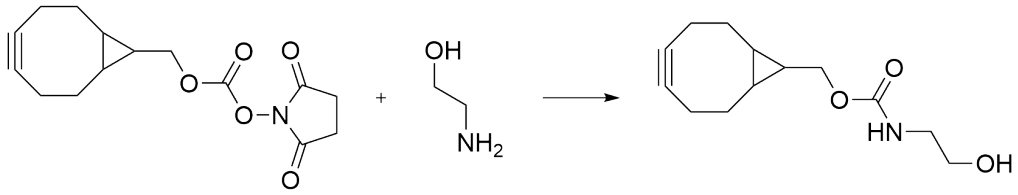

Figure 24: Reaction scheme for the synthesis of 9-bicyclo[6.1.0]non-4-ynylmethyl N-(2-hydroxyethyl)carbamate

Table 4: Reagents used in the synthesis of 9-bicyclo[6.1.0]non-4-ynylmethyl N-(2-hydroxyethyl)carbamate

synthesis	substance	M [g/mol]	m [g]	n [mmol]	V [ml]	ρ [g/ml]	equiv.
RL3	**A**	291.3	0.005	0.017	-	-	1.00
	B	61.08	0.001	0.017	0.001	1.012	1.00
RL5	**A**	291.3	0.050	0.172	-	-	1.00
	B	61.08	0.011	0.017	0.01	1.012	1.00
RL6	**A**	291.3	0.022	0.076	-	-	1.00
	B	61.08	0.005	0.076	0.005	1.012	1.00
RL8	**a**	291.3	0.020	0.070	-	-	1.00
	b	61.08	0.004	0.070	0.004	1.012	1.00
RL9	**a**	291.3	0.020	0.070	-	-	1.00
	b	61.08	0.004	0.070	0.004	1.012	1.00
a: (1R,8S,9s)-bicyclo[6.1.0]non-4-in-9-ylmethyl]-N-succinimidylcarbonate; b: ethanolamine							

In a glass vial, (1R,8S,9s)-bicyclo[6.1.0]non-4-in-9-ylmethyl]-N-succinimidylcarbonate was dissolved in 3 ml of dichloromethane (DCM), as seen in Table 4. Ethanolamine was added under vigorous stirring at room temperature. TLC controls were conducted (mobile phase: hexane/ethyl acetate 1:9) and the reaction was considered complete after 0.5 hours. The reaction was halted after exactly 1.5 hours, water was added, and the organic phase was subjected to extraction with DCM (3x). After drying the combined organic phases over Na_2SO_4, the product was filtered through cotton in a Pasteur pipette and transferred into a pointed flask for concentration under vacuum. ^{1}H-NMR measurements were performed. The obtained product (RL3), a white oily substance, corresponded to a 74% yield before purification.

In an attempt to replicate the results on a larger scale (RL5), the reaction was considered complete after 20 hours by obtaining TLC controls. The workup was conducted as previously described, and

the analytical data did not exhibit significant differences. Unfortunately, during Biotage column chromatography, a practical error occurred 10% ethyl acetate in hexane was employed instead of the intended 10% hexane in ethyl acetate. This led to a substantial loss of product, resulting in 16 mg worth of product corresponding to a 13% yield.

The reaction was repeated three additional times (RL6/8/9), and in each instance, the reaction was considered complete after 0.5 hours. The products of these reactions (RL6, RL8, and RL9) underwent purification through silica gel using a Pasteur pipette for column chromatography. The remaining products were obtained in yields presented in Table 5.

Table 5: Yields of 9-bicyclo[6.1.0]non-4-ynylmethyl N-(2-hydroxyethyl)carbamate

synthesis	m [mg]	yield [%]
RL3	5.00	74*
RL5	50.00	13
RL6	22.00	70
RL8	20.30	45
RL9	20.30	56
* before purification		

3.5. Synthesis of 2-(9-bicyclo[6.1.0]non-4-ynylmethoxycarbonylamino)ethyl 4-methyl-benzenesulfonate

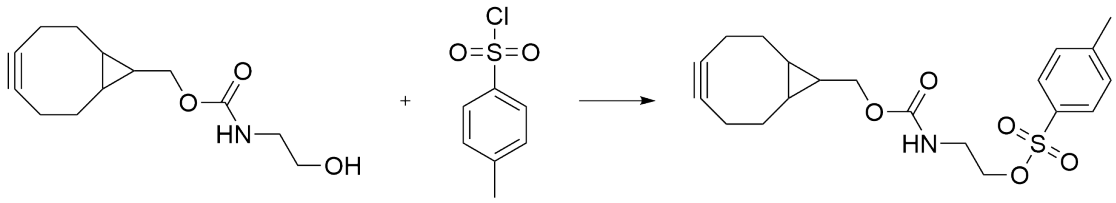

Figure 25: Reaction scheme for the synthesis of 2-(9-bicyclo[6.1.0]non-4-ynylmethoxycarbonyl-amino)ethyl 4-methyl-benzenesulfonate

Table 6: Reagents used in the synthesis of 2-(9-bicyclo[6.1.0]non-4-ynylmethoxycarbonylamino)ethyl 4-methyl-benzenesulfonate

synthesis	substance	M [g/mol]	m [g]	n [mmol]	V [ml]	ρ [g/ml]	equiv.
RL4	RL3	237.30	0.003	0.013	-	-	1.00
	pyridine	79.10	0.002	0.025	0.002	0.98	2.00
	p-TsCl	190.64	0.002	0.013	-	-	1.00
RL7	RL6	237.30	0.013	0.053	-	-	1.00
	pyridine	79.10	0.008	0.105	0.008	0.98	2.00
	p-TsCl	190.64	0.010	0.053	-	-	1.00
RL17	RL8	237.30	0.007	0.031	-	-	1.00
	TEA	101.19	0.006	0.062	0.009	0.73	2.00
	p-TsCl	190.64	0.006	0.031	-	-	1.00

As seen in Table 6, the products derived from reactions RL3 and RL6 were employed in two distinct attempts for the tosylation reaction (RL4 and RL7). Initially, the compound was dissolved in DCM, and under vigorous stirring, pyridine was added, followed by the introduction of p-TsCl. TLC controls (mobile phase: hexane/ethyl acetate 1:4) were conducted over a three-hour period. After allowing the solution to stir overnight, the reaction was terminated after 22 hours. Water was added, and the organic phase underwent extraction with DCM (3x). Following the drying of the organic phase with Na_2SO_4 and filtration into a pointed flask, the product was concentrated under reduced pressure. Subsequently, an ^{1}H-NMR measurement was conducted, revealing no isolated product from this reaction.

Utilizing the product RL8, the approach was repeated (RL17), replacing the base pyridine with triethylamine. This modification is based on findings elaborated in chapter 3.6. However, this attempt did not yield product.

3.6. Synthesis of 2-aminoethyl 4-methyl-benzenesulfonate

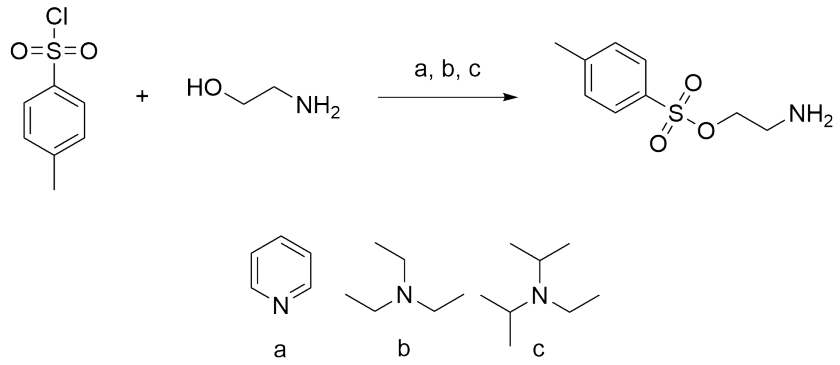

Figure 26: Reaction scheme for the synthesis of 2-aminoethyl-4-methyl-benzenesulfonate

Table 7: Reagents used in the synthesis of 2-aminoethyl-4-methyl-benzenesulfonate

synthesis	substance	M [g/mol]	m [g]	n [mmol]	V [ml]	ρ [g/ml]	equiv.
RL10,13	**d**	190.65	0.050	0.262	-	-	1
	a	79.10	0.042	0.525	0.042	0.980	2
	e	61.08	0.016	0.262	0.016	1.010	1
RL11,14	**d**	190.65	0.050	0.262	-	-	1
	c	129.24	0.068	0.525	0.091	0.068	2
	e	61.08	0.016	0.262	0.016	1.010	1
RL12,15	**d**	190.65	0.050	0.262	-	-	1
	b	101.19	0.053	0.525	0.073	0.730	2
	e	61.08	0.016	0.262	0.016	1.010	1
a: pyridine; b: TEA; c: N-N-diisopropylethylamine; d: p-TsCl; e: ethanolamine							

In three separate glass vials, p-TsCl was dissolved in DCM, as detailed in Table 7. Subsequently, each vial received one of three bases: pyridine (a), triethylamine (TEA) (b), or N,N-diisopropylethylamine (c), as indicated in Table 6. The mixtures were stirred for 10 min. Ethanolamine was introduced under vigorous stirring. The progression of the reaction was monitored using TLC (mobile phase: hexane/ethyl acetate 1:4). The solution was stirred for 20 hours, quenched with water, and subjected to extraction with DCM (3x). The organic phase was dried with Na_2SO_4, filtered, and then evaporated. Subsequent measurements of ^{1}H-NMR and infrared spectroscopy were conducted. However, no product was synthesized using this procedure.

Table 8: Reagents used in the synthesis of synthesis of 9-bicyclo[6.1.0]non-4-ynylmethyl N-(2-hydroxyethyl)carbamate

synthesis	substance	M [g/mol]	m [g]	n [mmol]	V [ml]	ρ [g/ml]	equiv.
RL16	**RL15**	215.27	0.046	0.214	-	-	1.00
	a	291.30	0.062	0.214	-	-	1.00
a: (1R,8S,9s)-bicyclo[6.1.0]non-4-in-9-ylmethyl]-N-succinimidylcarbonate							

As presented in Table 8, RL15 was used to perform the next step of the synthesis, the attachment of 2-aminoethyl-4-methyl-benzenesulfonate to the commercially available (1R,8S,9s)-bicyclo[6.1.0]non-4-in-9-ylmethyl]-N-succinimidylcarbonate. RL15 was dissolved in DCM and the BCN compound was added. The reaction was monitored via TLC (mobile phase: hexane/ethyl acetate 1:3). Following an overnight stirring period, the TLC controls exhibited no observable changes. The reaction temperature was then elevated to approximately 50-80 degrees. After an additional two hours, the reaction was terminated, quenched with water, and subjected to extraction with DCM (3x). The organic phase was dried using Na_2SO_4 and filtered. After the concentration of the product under vacuum, an ^{1}H-NMR measurement was conducted, revealing an unsuccessful reaction.

3.7. Synthesis of 1-(isobutylsulfonyl)-4-methylbenzene

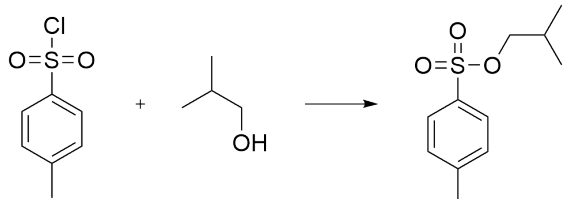

Figure 27: Reaction scheme for the synthesis of 1-(isobutylsulfonyl)-4-methylbenzene

Table 9: Reagents used in the synthesis of1-(isobutylsulfonyl)-4-methylbenzene

synthesis	substance	M [g/mol]	m [g]	n [mmol]	V [ml]	ρ [g/ml]	equiv.
RL18	p-TsCl	190.64	0.050	0.262	-	-	1.00
	TEA	101.19	0.053	0.525	0.053	0.73	2.00
	Propanol	60.10	0.016	0.262	0.020	0.80	1.00

As indicated in Table 9, 2-propanol and TEA were stirred in DCM, while simultaneously p-TsCl was diluted in DCM and introduced into the mixture. Ongoing TLC controls (mobile phase: hexane/ethyl acetate in various ratios) were performed. After stirring for 24 hours, the reaction was halted, water was added to the solution, and the resulting mixture was subjected to extraction with DCM (3x). The organic phases were dried using Na_2SO_4, filtered, and then concentrated under reduced pressure. Analysis of the ^{1}H-NMR spectrum and HRMS measurement indicated the absence of product from this reaction.

3.8. Synthesis of N-phenethyl-p-toluenesulfonamide

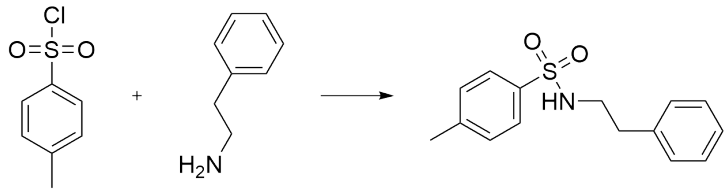

Figure 28: Reaction scheme for the synthesis of N-phenethyl-p-toluenesulfonamide

Table 10: Reagents used in the synthesis of N-phenethyl-p-toluenesulfonamide

synthesis	substance	M [g/mol]	m [g]	n [mmol]	V [ml]	ρ [g/ml]	equiv.
RL19	p-TsCl	190.64	0.050	0.262	-	-	1.00
	TEA	101.19	0.053	0.525	0.053	0.73	2.00
	PEA	121.18	0.032	0.262	0.033	0.96	1.00

Simultaneously the same reaction was performed using phenylethylamine instead of 2-propanol, as seen in Table 10. In this case, ^{1}H-NMR and HRMS indicated a successful S_N2-reaction.

3.9. Synthesis of 2-(N-tert-butoxycarbonylamino)ethanol

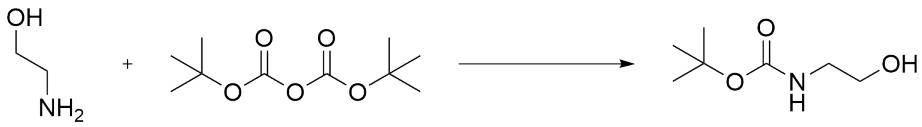

Figure 29: Reaction scheme for the synthesis of 2-(N-tert-butoxycarbonylamino)ethanol

Table 11: Reagents used in the synthesis of 2-(N-tert-butoxycarbonylamino)ethanol

synthesis	substance	M [g/mol]	m [g]	n [mmol]	V [ml]	ρ [g/ml]	equiv.
RL20	**a**	61.08	0.020	0.327	0.02	0.101	1
	b	218.25	0.072	0.327	0.075	0.950	2
RL22	**a**	61.08	0.281	4.600	0.278	0.101	1
	b	218.25	1.004	4.600	1.053	0.950	2
a: ethanolamine; b: Boc_2O							

Boc_2O was dissolved in DCM and subsequently ethanolamine was added, as presented in Table 11. TLC controls were conducted (mobile phase: methanol). The reaction was terminated after stirring at room temperature for 30 min and the solution was quenched with water. After extracting with DCM (3x), the organic layers were consolidated, dried over Na_2SO_4, filtered, and then concentrated under reduced pressure. This procedure yielded a clear oil, which was not subjected to further purification. HRMS and ^{1}H-NMR measurements were performed and suggested a successful N-Boc-protection.

For a larger-scale synthesis (RL22) and in a solvent-free environment, the same reaction was replicated. This product, too, was not purified for subsequent small-scale reactions.

3.10. Synthesis of 2-(tert-butoxycarbonylamino)ethyl-4-methylbenzenesulfonate

Figure 30: Reaction scheme for the synthesis of 2-tert-butoxycarbonylamino)ethyl-4-methylbenzenesulfonate

Table 12: Reagents used in the synthesis of 2-tert-butoxycarbonylamino)ethyl-4-methylbenzenesulfonate

synthesis	substance	M [g/mol]	m [g]	n [mmol]	V [ml]	ρ [g/ml]	equiv.	solvent
RL23	**RL22**	161.19	0.100	0.620	0.100	-	1	DCM
	p-TsCl	190.64	0.118	0.620	-	-	1	
	TEA	101.19	0.126	1.241	0.172	0.730	2	
RL24	**RL22**	161.19	0.100	0.620	-	-	1	ACN
	p-TsCl	190.64	0.118	0.620	-	-	1	
	TEA	101.19	0.126	1.241	0.172	0.730	2	
RL25	**RL22**	161.19	0.100	0.620	-	-	1	DCM
	p-TsCl	190.64	0.118	0.620	-	-	1	
	pyridine	79.1	0.098	1.241	0.100	0.989	2	
RL26	**RL22**	161.19	0.100	0.620	-	-	1	THF
	p-TsCl	190.64	0.118	0.620	-	-	1	
	TEA	101.19	0.126	1.241	0.172	0.730	2	
RL27	**RL22**	161.19	0.100	0.620	-	-	1	THF
	p-TsCl	190.64	0.118	0.620	-	-	1	
	NaOH	40	0.0496	1.241	0.620	0.080	2	

As outlined in Table 11, RL22 was dissolved in either dichloromethane (DCM), acetonitrile (ACN), or tetrahydrofuran (THF). Upon addition of TEA, pyridine, or sodium hydroxide (NaOH), p-TsCl was introduced to the mixture. The progress of the reactions was monitored via TLC (mobile phase: hexane/ethyl acetate 1:4) and maintained at a temperature range from 0 °C to room temperature, stirring continuously for one week. Upon termination of the reactions, new spots appeared on TLC. Water was added to each vial, and after extracting the aqueous phases with DCM (3x), the combined organic phases were dried over Na_2SO_4, filtered, and subsequently evaporated under reduced pressure. Measurements involving ^{1}H-NMR and HRMS were conducted for analysis.

4. Results and Discussion

4.1. Synthesis of the small molecule 3-[2-(4-Fluorobenzyl)imidazo[2,1-b][1,3]thiazol-6-yl]-2H-chromen-2-one

4.1.1. Synthesis of 3-aryl-2-chloropropanal

The synthesis attempts for 3-aryl-2-chloropropanal, the first intermediate of the small molecule synthesis, proved to be unsuccessful. The initial approach implemented by Kutonova et al.[49] utilizing TsOH in the diazotization process encountered significant challenges in subsequent steps, particularly in the Meerwein reaction. The choice of TsOH as the diazotization agent caused problems related to issues based on counterion incompatibility during subsequent reactions with acrolein diethyl acetal/$CuCl_2$, as described in Figure 31 (A). To address this, a literature search revealed successful alternatives using HCl instead. This aimed to mitigate any counterion-related obstacles that may have appeared during the synthesis process.

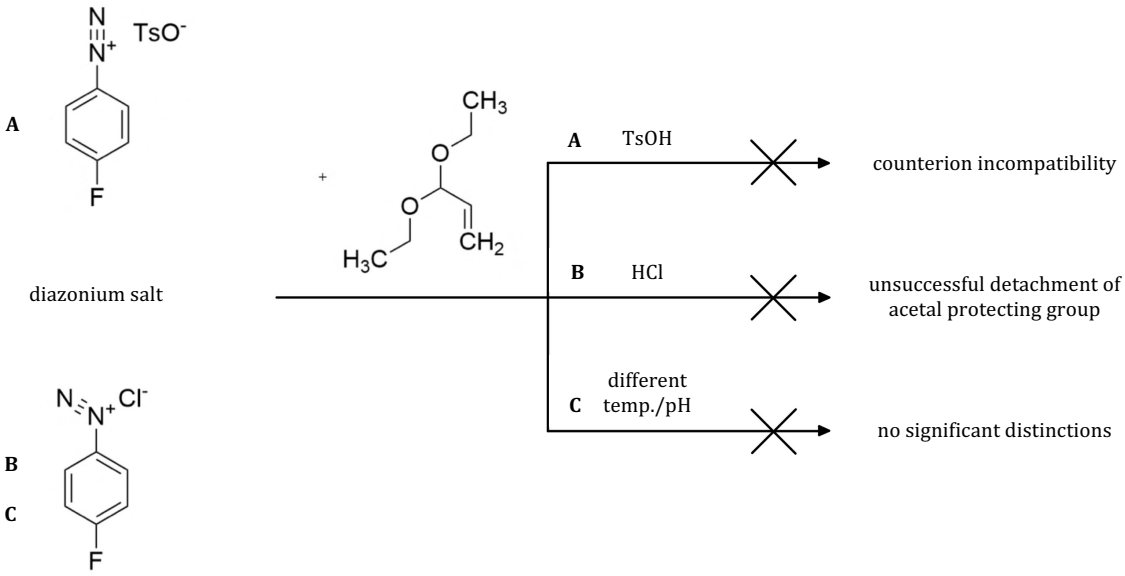

Figure 31: Experiments conducted in the synthesis of 3-aryl-2-chloropropanal

The new approach followed the procedure according to Krasavin et al.[50], with the only distinction being the utilization of acrolein diethyl acetal instead of acrolein, as the latter is no longer commercially available due to toxicity. The evaluation of raw ^{1}H-NMR measurements proved to be difficult, as there were numerous impurity peaks. Therefore, the product obtained from synthesis rola, a brown oil, was purified using the automated column chromatography Biotage.

Regardless of the purification process, the collected fractions did not reveal the anticipated product when measured via ^{1}H-NMR and HRMS, as described in Figure 31 (B).

In an attempt to adhere more closely to another literature protocol[37], variations were introduced into the synthesis procedure, as seen in Figure 31 (C). Two notable modifications were implemented: to neutralize the diazonium salt solution by adding $NaHCO_3$ to achieve a pH within the range of 6 to 7. Additionally, MgO was incorporated into the reaction mixture. The influence of different temperature settings (60, 70, and 80 °C) was also investigated to optimize the reaction conditions. The ^{1}H-NMR spectra did not present significant distinctions across temperature variations. Despite these adjustments, both sets of reactions failed to yield the desired product. It is reasonable to attribute this failure to the requirement of acidic conditions for the detachment of acetal protecting groups from acrolein.

^{1}H-NMR measurements across all attempts revealed the presence of numerous impurities, making the identification of anticipated product peaks challenging. The HRMS results further underscored the complexity of the reaction outcomes, indicating an excess of one hydrogen in the product compared to the expected molecular formula. This discrepancy suggests potential issues such as unexpected hydrogenation, reduction, or other side reactions during the synthesis. The exact cause could not be determined.

In conclusion, despite careful considerations and adjustments in reaction conditions, the synthesis of 3-aryl-2-chloropropanal proved to be difficult. The challenges encountered, including issues with diazotization and subsequent reactions, impurity-laden ^{1}H-NMR spectra, and unexpected HRMS data, underscore the sensitivity of this synthetic route. Further investigations, potentially involving the prior deprotection of the acrolein diethyl acetal, may be necessary to overcome these challenges and achieve the successful synthesis of the target compound.

4.2. First synthesis of the crosslinker 2-(9-bicyclo[6.1.0]non-4-ynylmethoxycarbonylamino)ethyl 4-methyl-benzenesulfonate

4.2.1. Synthesis of 9-bicyclo[6.1.0]non-4-ynylmethyl N-(2-hydroxyethyl)carbamate

In the preliminary small-scale attempt (RL3), the reaction progressed swiftly, turning the mixture white within 0.5 hours, and the product ultimately appeared as a white oil. The ^{1}H-NMR spectra exhibited the anticipated product peaks. The individual spectra are found in the Appendix

displaying peaks and integrations in more detail. As seen in Figure 32, (A) displays the ^{1}H-NMR peaks of RL3 compared to the starting BCN compound. Looking at (A), the distinct broad singlet at approximately 5.0 ppm and the triplets for H 15/16 indicated a successful reaction with the amine end of ethanolamine. Due to the limited yield (3 mg), this product was utilized directly in a subsequent small-scale reaction without prior purification.

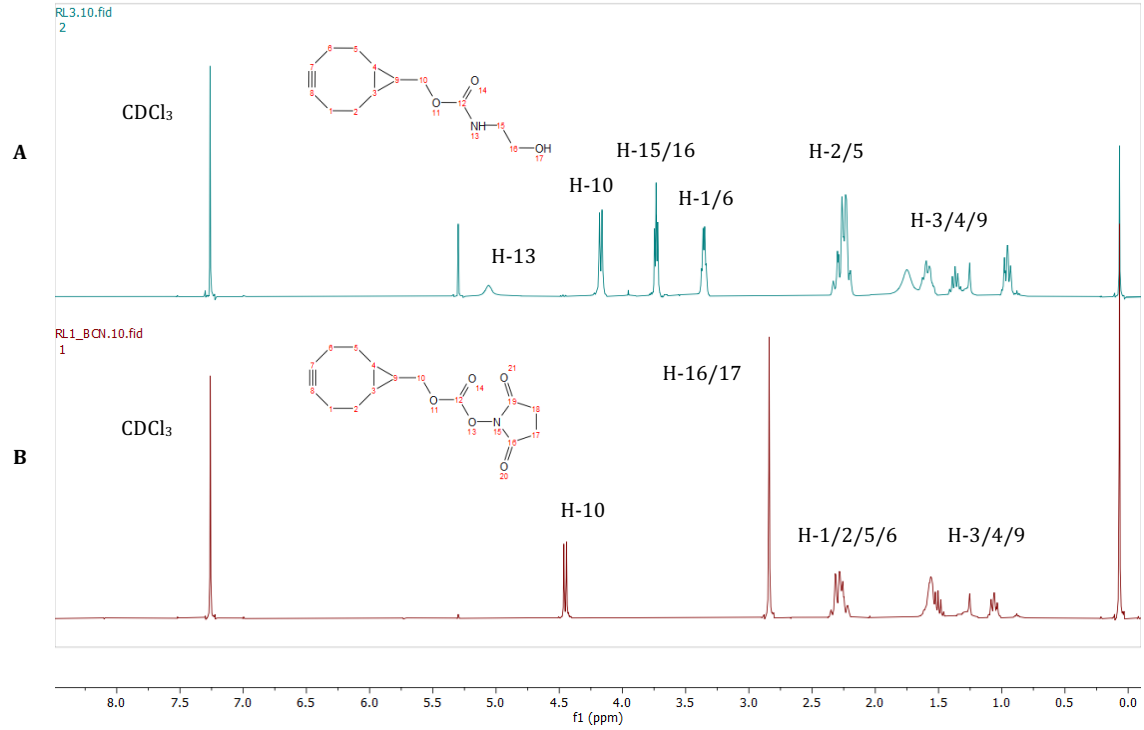

Figure 32: ^{1}H-NMR spectra of RL3 (A) and (1R,8S,9s)-bicyclo[6.1.0]non-4-in-9-ylmethyl]-N-succinimidylcarbonate (B)

Scaling up the reaction (RL5) resulted in the mixture turning clear within 0.5 hours. The reaction was deemed complete after 20 hours as TLC controls confirmed. The analytical data did exhibit similar results as the previous attempt. However, a practical error during Biotage column chromatography resulted in a significant product loss, with only 16 mg recovered, yielding 13%. During calibration, the mobile phase was incorrectly set to 10% ethyl acetate in hexane instead of 10% hexane in ethyl acetate. This misalignment led to a significant portion of the product being discarded.

Repetition of the reaction (RL6/8/9) mirrored the initial attempt (RL3) in slightly larger scale and ^{1}H-NMR measurements presented very similar results, which are included in the Appendix. Except for RL9, showing significantly more impurities despite the exact same procedure. Purification of the products from these repetitions using a pipette for silica gel column chromatography yielded the amounts listed in the table below. However, subsequent reactions

(RL4, RL7, and RL17) with the purified products revealed unexpected impurities, as evidenced by TLC controls displaying three spots instead of one. This discrepancy was perplexing, given that during the purification process, TLC controls undoubtedly indicated a single spot. This inconsistency may hint at stability issues of the product obtained from this reaction.

Initially appearing as white oils, RL6/8/9 products solidified upon storage for a few days after purification. This observation suggests potential changes in the physical properties of the compounds over time. The occurrence of impurities in subsequent reactions, despite purification efforts, warrants further investigation into the stability and reactivity of the purified products. Additional optimizations to the synthetic route may be necessary to address these unexpected outcomes and ensure the reliability of the final target compound.

The yields obtained from all reactions are listed in Table 13. The actual yields are likely to have been significantly lower, as there still were peaks of impurities in the ^{1}H-NMR spectra after purification efforts, which presumably could be referenced to side-reactions during incorrect storage.

Table 13: Yields and appearance of 9-bicyclo[6.1.0]non-4-ynylmethyl N-(2-hydroxyethyl)carbamate

synthesis	m [mg]	appearance	yield [%]
RL3	5.00	white oil	74**
RL5	50.00	white oil	13
RL6	22.00	white oil*	70
RL8	20.30	white oil*	45
RL9	20.30	white oil*	56
* white solid substance after purification			
** before purification			

4.2.2. Synthesis of 2-(9-bicyclo[6.1.0]non-4-ynylmethoxycarbonylamino)ethyl 4-methyl-benzenesulfonate

The preliminary attempts (RL4 and RL7), conducted with small quantities of the products derived from reactions RL3 and RL6, primarily aimed to assess the validity of the chosen reaction approach and to evaluate any reactivity between the compounds. However, subsequent ^{1}H-NMR and HRMS analysis revealed no isolated product from this reaction.

A compelling aspect emerged during the attempted tosylation reactions using products from previous syntheses (RL3, RL6, and RL8): potential stability issues of the intermediates. As discussed in 4.2.1, the purification through column chromatography was successful. However, the

subsequent TLC analysis during the tosylation attempts uncovered the presence of multiple spots. This unexpected outcome raises questions regarding the stability of the intermediates and suggests potential transformations occurring prior to or during this synthesis procedure. This could be indicative of instability of the intermediates due to specific reaction conditions employed or to incorrect storage.

The lack of isolated product in RL4, despite employing the base pyridine, indicates potential challenges in the reaction conditions or reagent compatibility. The replacement of pyridine with triethylamine (RL17), based on previous insights discussed in 4.3.1, also did not result in the desired product. This suggests that the tosylation reaction for this specific substrate requires further optimization or alternative conditions to achieve successful transformation. Additional investigations into the choice of base, reaction time and temperature, or potential side reactions due to incorrect storage may be necessary to overcome the observed difficulties in tosylating the intermediates.

4.3. Second synthesis of the crosslinker 2-(9-bicyclo[6.1.0]non-4-ynylmethoxycarbonylamino)ethyl 4-methyl-benzenesulfonate

4.3.1. Synthesis of 2-aminoethyl 4-methyl-benzenesulfonate

The use of the commercially available (1R,8S,9s)-Bicyclo[6.1.0]non-4-in-9-ylmethyl]-N-succinimidylcarbonate in small scale reactions was neither considered efficient nor cost-effective, prompting to rethink the synthesis strategy. Ethanolamine and p-TsCl were available at a significantly lower cost point and substantially higher quantity. The chosen approach involved the conjugation of ethanolamine with p-TsCl under basic conditions, aiming to minimize waste associated with the BCN compound and mitigate potential stability concerns.

Three sterically hindered bases—pyridine, triethylamine, and N-N-diisopropylethylamine—were investigated for their reactivities and properties in the reaction with p-TsCl and ethanolamine. None of the approaches yielded the desired product. Notably, the use of pyridine resulted in a higher number of side-product peaks observed in the ^{1}H-NMR spectra.

Interpreting the analytical data posed challenges due to the different potential outcomes of the synthesis: either the amine or the hydroxyl group of ethanolamine could react with the tosylate. As a result, the HRMS measurement became inconclusive, and the chemical shifts in the ^{1}H-NMR spectra were remarkably similar.

To gain additional insights, IR measurements were pursued and are included in the Appendix. As presented in Figure 33, the IR spectrum of RL15 was compared to spectra of ethanolamine, ethanol and p-TsCl to evaluate distinct O-H stretching bands known to be found at around 3700 to 3500 cm^{-1}.[51] A notable variation in the shape of O-H bands between (A) and (B) in comparison to the distinctive band in (C) was observed. The N-H band in (B), indicative of a primary amine, was anticipated in RL15 and is commonly encountered within this range (up to 3500 cm^{-1}). The similarity between the peak in (A) and that in (B) was evident. The C-H bands of the aromatic ring were identified in (A) within the range of 1800 to 1300 cm^{-1}. Peaks in the range of 1300 to 500 cm^{-1} were expected to exhibit a more rounded and broader appearance, representative of S-O-R. S=O bands can typically be found ranging from 1410 to 1380 cm^{-1}, as demonstrated in (D). However, these peaks were not distinctly identified in (A), likely attributable to distortions caused by impurities. In conclusion, the infrared results did not provide sufficient clarity for result evaluation, as the O-H peak was likely distorted due to the presence of the amine.

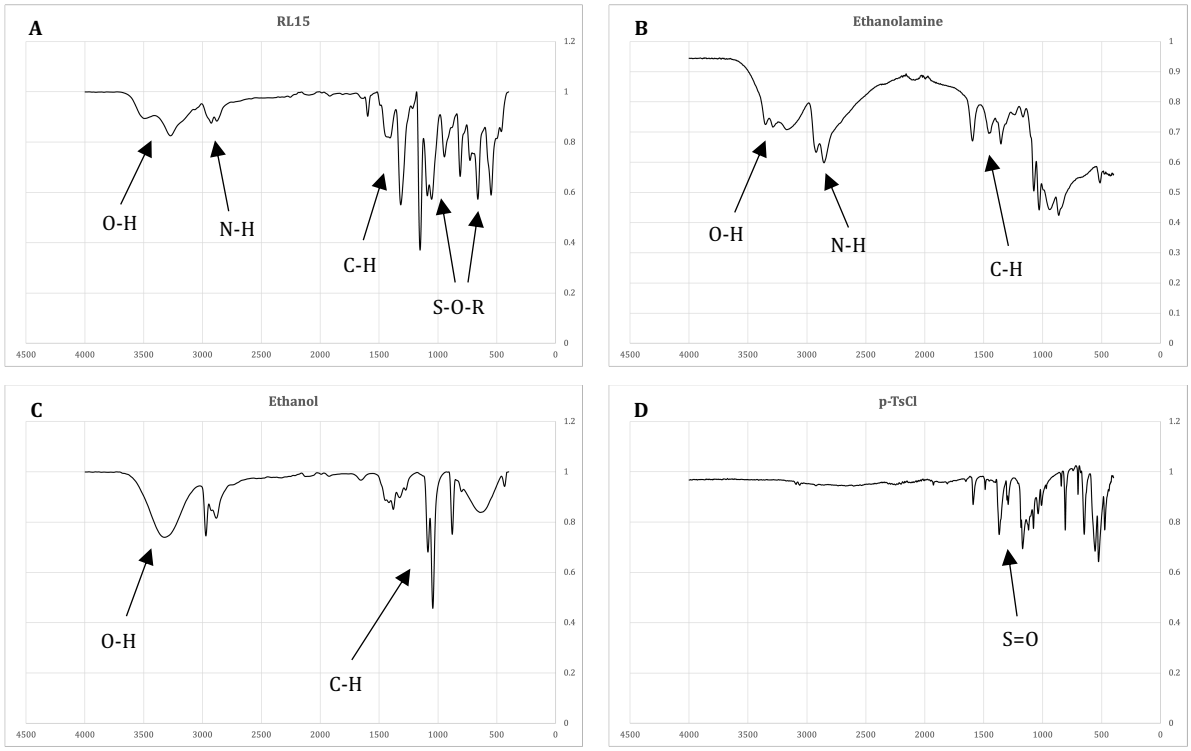

Figure 33: IR spectra conducted in the synthesis of 2-aminoethyl 4-methyl-benzenesulfonate: (A) RL15; (B) ethanolamine; (C) ethanol; (D) p-TsCl

The lack of desired product in all reaction scenarios suggests challenges in achieving successful conjugation between p-TsCl and the hydroxyl group of ethanolamine under these conditions. The higher occurrence of side-products in the reaction with pyridine emphasizes the importance of base selection in influencing the outcomes. Further explorations of alternative reaction conditions or utilization of protecting groups proved necessary to overcome these obstacles.

4.3.2. Synthesis of 1-(isobutylsulfonyl)-4-methylbenzene and N-phenethyl-p-toluenesulfonamide

Investigating the reactivity of ethanolamine, two syntheses were explored to conduct further information, aiming to distinguish whether the hydroxyl group exhibits greater reactivity than the amine group. The reaction of p-TsCl with propanol did not yield the expected product according to analytical data found in the Appendix. In contrast, ^{1}H-NMR and HRMS data of the reaction with phenylethylamine, as presented in Figures 34/35, indicated a successful reaction. The impurity peaks most probably can be assigned to remains of TEA.

HRMS (ESI): (m/z) = $[M + Na]^+$ calculated for $C_{15}H_{17}NNaO_2S$: 298.0872, found: 298.09

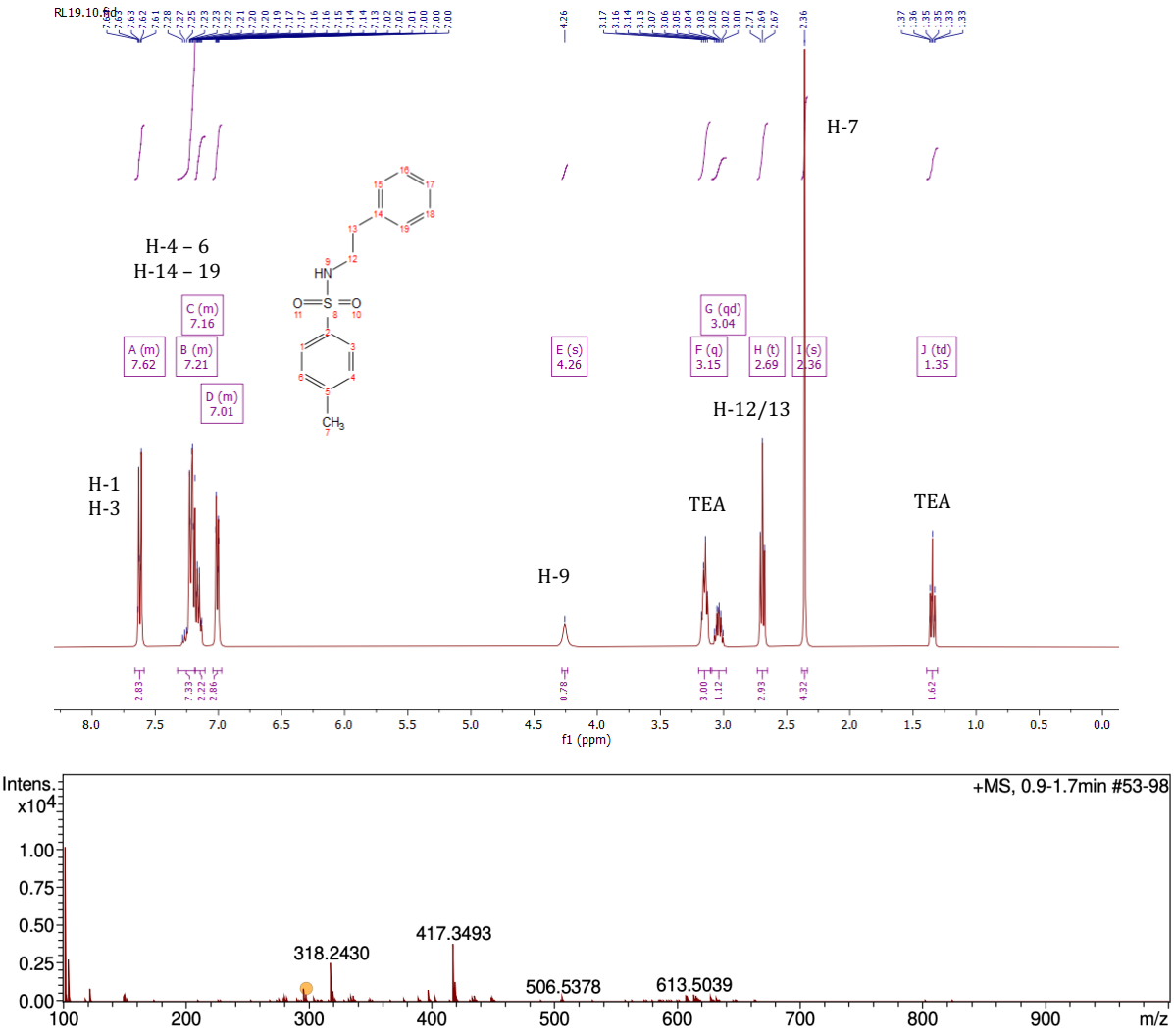

Figure 34: ^{1}H-NMR and HRMS spectrum of RL19

This observation confirms the suspicion that the amine end of ethanolamine might possess higher reactivity than expected and therefore interfere with the reactivity of the hydroxyl group.

4.4. Third synthesis of the crosslinker 2-(9-bicyclo[6.1.0]non-4-ynylmethoxycarbonyl-amino)ethyl-4-methyl-benzenesulfonate

4.4.1. Synthesis of 2-(N-tert-butoxycarbonylamino)ethanol

To prevent undesired reactions, it was established in previous experiments that implementing a protecting group to the amine end of ethanolamine was necessary. A BOC protecting group was introduced (RL20) yielding 86%, as seen in ^{1}H-NMR and HRMS spectra presented in Figure 35. The individual spectra are found in the Appendix displaying peaks and integrations in more detail. The carboxyl peaks at 1-1.5 ppm represent the hydrogen atoms of the BOC protecting group.

HRMS (ESI): (m/z) = $[M + Na]^+$ calculated for $C_7H_{15}NNaO_3$: 184.0944, found: 184.0955

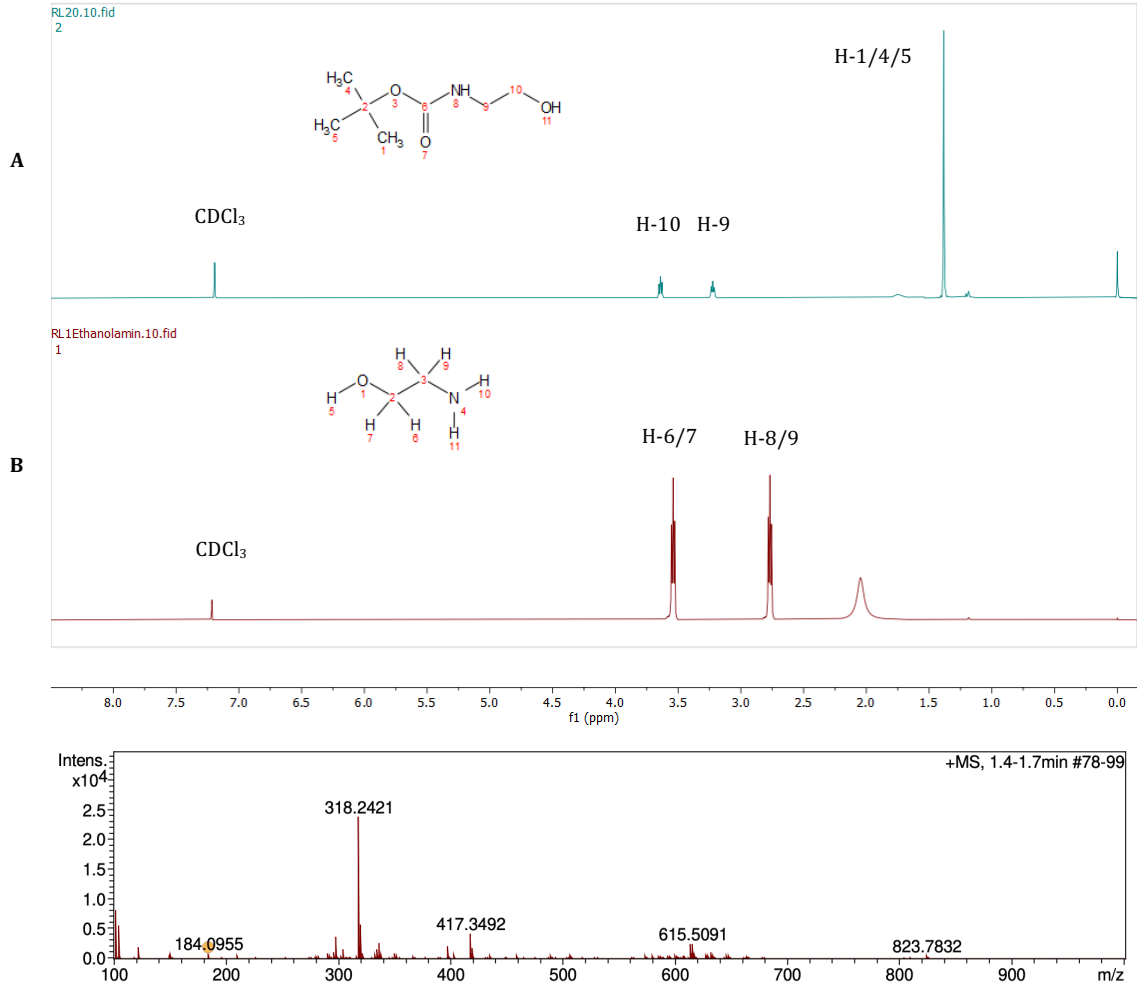

Figure 35: ^{1}H-NMR of (A) RL20 and (B) ethanolamine; HRMS spectrum of RL20

Following literature[47] suggestions, the reaction was replicated in larger scale and in solvent-free environment (RL22), resulting in 595.4 mg of N-Boc-ethanolamine corresponding to a yield of 80%. The analytical data obtained from both reactions, enclosed in the Appendix section, was nearly identical. In both instances, a transparent oil was obtained, and the resulting products were used for subsequent tosylation reactions. Purification was omitted since ^{1}H-NMR analysis did not reveal significant impurity peaks. It is of interest to note that the reaction was considered complete by TLC controls after just 30 min, a by far shorter duration than suggested in the literature.

4.4.2. Synthesis of 2-(tert-butoxycarbonylamino)ethyl-4-methylbenzenesulfonate

The product obtained from reaction RL22 served as the starting material for the subsequent reactions. In five distinct approaches, the tosylation reaction was conducted to assess potentially favourable conditions. Utilizing three different bases – triethylamine, pyridine and NaOH – the reactions were executed in various polar aprotic solvents, involving DCM, ACN and THF. The temperature was maintained at 0 °C for the first 10 hours of the reaction, gradually reaching room temperature over the week-long stirring period.

HRMS measurements consistently revealed the formation of the anticipated product across all procedures, varying in the number of impurities, as affirmed by ^{1}H-NMR spectra. As the extent of side-products was substantially high across all approaches and the obtained product amounts were relatively small, this process should preferably be repeated in sufficiently higher scale to make purification efforts more efficient.

Interestingly, the choice of solvent did not have substantial influence on the overall outcome. However, in regard of the choice of base, triethylamine emerged as the more favourable option. Employing pyridine did result in a higher occurrence of impurities and the yellow colour of the product, in contrast to the otherwise white products, underscored this discrepancy. The utilisation of an aqueous solution of NaOH was suggested by Ouchi et al.[52] and was included to get a broader spectrum of results. One rather unconventional approach involved using an aqueous NaOH solution. This method first raised concerns due to the potential reactivity of p-toluenesulfonyl chloride with water, as it is known for resulting in the formation of hydrochloric acid, potentially disrupting the tosylation reaction. Despite these apprehensions, HRMS measurements confirmed the successful formation of the targeted product in this experiment.

This underscores the importance of exploring unconventional methods and comparing it to established conditions to provide insights for further optimizations.

Ultimately, this experiment revealed a promising direction for future studies. Further upscaled reactions using TEA and maintaining the temperature at a constant 0 °C is anticipated to yield the desired product. It is important to note that extensive purification efforts will most certainly be necessary. Moreover, to improve this process, different suggestions concerning the workup were found in literature[53], including washing steps with solvent mixtures such as H_2O/pyridine (6:1) and H_2O /37% aq. HCl (4:1) prior to the drying process. These additional steps might enhance the purity of the final product and should be considered for the optimization of the entire synthesis strategy.

5. Conclusion

This work aimed to establish a synthesis strategy for a small molecule and a bioorthogonal linker, both specifically tailored for fluorine-18 labelling. The first step of the 3-step synthesis of 3-[2-(4-fluorobenzyl)imidazo[2,1-b][1,3]thiazol-6-yl]-2H-chromen-2-one required the formation of a diazonium salt followed by its reaction with acrolein diethyl acetal, which first faced challenges concerning the diazotization. A thorough literature search revealed a more promising procedure, yet reaction issues with acrolein diethyl acetal persisted. A variety of temperature settings and pH-levels were tested, setting the groundwork for future experiments to achieve the first intermediate 3-aryl-2-chloropropanal.

The focus was then shifted to the synthesis of the crosslinker containing a BCN compound providing a clickable handle for a subsequent reaction with 5'-C3-azide. Experiments concerning the reactivity of p-TsCl and ethanolamine were conducted and presented the necessity of a BOC-protection of the amine end of ethanolamine. The BOC-protecting group was successfully established, followed by subsequent reactions for the second step of the 4-step synthesis, which provided promising results. In the process, the choice of the base utilized in the reaction was examined, showing that pyridine causes more impurities than triethylamine, despite literature predominantly suggesting the use of pyridine for this reaction.

The results of this master thesis offer solid groundwork for further experiments for the synthesis of both small molecules and therefore contributes to the development of ^{18}F-labelled radiopharmaceuticals.

6. Index of abbreviations

2-[^{18}F]FDG	(2-[^{18}F]fluoro-2-deoxy-D-glucose)
ACN	acetonitrile
BCN	bicyclo[6.1.0]non-4-yne
BOC	tert-butyloxycarbonyl
Boc_2O	di-tert-butyldicarbonate
CO_2	carbon dioxide
$CuCl_2$	copper chloride
DCM	dichloromethane
DNA	deoxyribonucleic acid
EtOH	ethanol
FETos	fluoroethyl tosylate
HCl	hydrochloric acid
HNO_2	nitrous acid
IEDDA	Inverse-Electron Demand Diels-Alder
IR	infrared spectroscopy
MDK	Midkine growth factor
MgO	magnesium oxide
MS	mass spectrometry
Na_2SO_4	sodium sulfate
$NaHCO_3$	sodium bicarbonate
$NaNO_2$	sodium nitrite
NMR	nuclear magnetic resonance
Nu	nucleophile
PEA	phenylethylamine
PET	positron emission tomography
PG	prosthetic group
p-TsCl	p-toluenesulfonyl chloride
p-TsOH	p-toluenesulfonic acid
SFB	N-succinimidyl 4-fluorobenzoate
SPAAC	Strain-Promoted Alkyne Azide Cycloaddition
SPECT	single-photon emission computed tomography
TEA	triethylamine
TFA	trifluoroacetic acid
TLC	thin layer chromatography

7. List of References

1. Muramatsu T. Midkine, a heparin-binding cytokine with multiple roles in development, repair and diseases. *Proc Jpn Acad Ser B Phys Biol Sci*. 2010;86(4):410-425. doi:10.2183/pjab.86.410
2. Filippou PS, Karagiannis GS, Constantinidou A. Midkine (MDK) growth factor: a key player in cancer progression and a promising therapeutic target. *Oncogene*. 2020;39(10):2040-2054. doi:10.1038/s41388-019-1124-8
3. Jones DR. Measuring midkine: the utility of midkine as a biomarker in cancer and other diseases. *Br J Pharmacol*. 2014;171(12):2925-2939. doi:10.1111/bph.12601
4. Muramatsu T. Structure and function of midkine as the basis of its pharmacological effects. *Br J Pharmacol*. 2014;171(4):814-826. doi:10.1111/bph.12353
5. Hao H, Maeda Y, Fukazawa T, et al. Inhibition of the Growth Factor MDK/Midkine by a Novel Small Molecule Compound to Treat Non-Small Cell Lung Cancer. Katoh M, ed. *PLoS ONE*. 2013;8(8):e71093. doi:10.1371/journal.pone.0071093
6. Matsui T, Ichihara-Tanaka K, Lan C, et al. Midkine inhibitors: application of a simple assay procedure to screening of inhibitory compounds. Published online 2010.
7. Fani M, Maecke HR, Okarvi SM. Radiolabeled Peptides: Valuable Tools for the Detection and Treatment of Cancer. *Theranostics*. 2012;2(5):481-501. doi:10.7150/thno.4024
8. Tai YF, Piccini P. Applications of positron emission tomography (PET) in neurology. *J Neurol Neurosurg Psychiatry*. 2004;75(5):669-676. doi:10.1136/jnnp.2003.028175
9. Charlton M. *New Routes to Fluorine-18 Radiolabelled Prosthetic Groups for Use in the Medical Imaging Technique - Positron Emission Tomography*. Thesis. Newcastle University; 2015. Accessed November 27, 2023. http://theses.ncl.ac.uk/jspui/handle/10443/2925
10. Muehllehner G, Karp JS. Positron emission tomography. *Phys Med Biol*. 2006;51(13):R117-137. doi:10.1088/0031-9155/51/13/R08
11. Cole EL, Stewart MN, Littich R, Hoareau R, Scott PJH. Radiosyntheses using Fluorine-18: the Art and Science of Late Stage Fluorination. *Curr Top Med Chem*. 2014;14(7):875-900.
12. Pichler V, Berroterán-Infante N, Philippe C, et al. An Overview of PET Radiochemistry, Part 1: The Covalent Labels 18F, 11C, and 13N. *J Nucl Med Off Publ Soc Nucl Med*. 2018;59(9):1350-1354. doi:10.2967/jnumed.117.190793
13. Shukla AK, Kumar U. Positron emission tomography: An overview. *J Med Phys Assoc Med Phys India*. 2006;31(1):13-21. doi:10.4103/0971-6203.25665
14. Born D van der, Pees A, J. Poot A, A. Orru RV, D. Windhorst A, J. Vugts D. Fluorine-18 labelled building blocks for PET tracer synthesis. *Chem Soc Rev*. 2017;46(15):4709-4773. doi:10.1039/C6CS00492J

15. Wadsak W, Mitterhauser M. Basics and principles of radiopharmaceuticals for PET/CT. *Eur J Radiol*. 2010;73(3):461-469. doi:10.1016/j.ejrad.2009.12.022
16. Hoh CK. Clinical use of FDG PET. *Nucl Med Biol*. 2007;34(7):737-742. doi:10.1016/j.nucmedbio.2007.07.001
17. Dollé F, Roeda D, Kuhnast B, Lasne M. Fluorine-18 Chemistry for Molecular Imaging with Positron Emission Tomography. In: *Fluorine and Health*. Elsevier; 2008:3-65. doi:10.1016/B978-0-444-53086-8.00001-1
18. Coenen HH, Elsinga PH, Iwata R, et al. Fluorine-18 radiopharmaceuticals beyond [18F]FDG for use in oncology and neurosciences. *Nucl Med Biol*. 2010;37(7):727-740. doi:10.1016/j.nucmedbio.2010.04.185
19. Hamacher K, Coenen HH, Stöcklin G. Efficient Stereospecific Synthesis of No-Carrier-Added 2-[18F]-Fluoro-2-Deoxy-D-Glucose Using Aminopolyether Supported Nucleophilic Substitution. *J Nucl Med*. 1986;27(2):235-238.
20. Rong J, Haider A, Liang S. Precision Radiochemistry for Fluorine-18 Labeling of PET Tracers. In: Szabó K, Selander N, eds. *Organofluorine Chemistry*. 1st ed. Wiley; 2021:397-425. doi:10.1002/9783527825158.ch12
21. Jacobson O, Kiesewetter DO, Chen X. Fluorine-18 Radiochemistry, Labeling Strategies and Synthetic Routes. *Bioconjug Chem*. 2015;26(1):1-18. doi:10.1021/bc500475e
22. Schirrmacher R, Wängler B, Bailey J, Bernard-Gauthier V, Schirrmacher E, Wängler C. Small Prosthetic Groups in 18F-Radiochemistry: Useful Auxiliaries for the Design of 18F-PET Tracers. *Semin Nucl Med*. 2017;47(5):474-492. doi:10.1053/j.semnuclmed.2017.07.001
23. Brooks AF, Makaravage KJ, Wright J, Sanford MS, Scott PJH. Fluorine-18 Radiochemistry. In: *Handbook of Radiopharmaceuticals*. John Wiley & Sons, Ltd; 2020:251-289. doi:10.1002/9781119500575.ch8
24. Vaidyanathan G, Zalutsky MR. Synthesis of N-succinimidyl 4-[18F]fluorobenzoate, an agent for labeling proteins and peptides with 18F. *Nat Protoc*. 2006;1(4):1655-1661. doi:10.1038/nprot.2006.264
25. Mäding P, Füchtner F, Wüst F. Module-assisted synthesis of the bifunctional labelling agent N-succinimidyl 4-[18F]fluorobenzoate ([18F]SFB). *Appl Radiat Isot*. 2005;63(3):329-332. doi:10.1016/j.apradiso.2005.03.005
26. Kniess T, Laube M, Brust P, Steinbach J. 2-Fluoroethyl tosylate – a versatile tool for building ^{18}F-based radiotracers for positron emission tomography. *MedChemComm*. 2015;6(10):1714-1754. doi:10.1039/C5MD00303B
27. Nymann Petersen I, Madsen J, Bernard Matthijs Poulie C, Kjær A, Manfred Herth M. One-Step Synthesis of N-Succinimidyl-4-[18F]Fluorobenzoate ([18F]SFB). *Molecules*. 2019;24(19):3436. doi:10.3390/molecules24193436

28. Meyer JP, Adumeau P, Lewis JS, Zeglis BM. Click Chemistry and Radiochemistry: The First 10 Years. *Bioconjug Chem*. 2016;27(12):2791-2807. doi:10.1021/acs.bioconjchem.6b00561
29. Li XG, Roivainen A, Bergman J, et al. Enabling [18F]-bicyclo[6.1.0]nonyne for oligonucleotide conjugation for positron emission tomography applications: [18F]-anti-microRNA-21 as an example. *Chem Commun*. 2015;51(48):9821-9824. doi:10.1039/C5CC02618K
30. Handula M, Chen KT, Seimbille Y. IEDDA: An Attractive Bioorthogonal Reaction for Biomedical Applications. *Molecules*. 2021;26(15):4640. doi:10.3390/molecules26154640
31. Baskin JM, Bertozzi CR. Bioorthogonal Click Chemistry: Covalent Labeling in Living Systems. *QSAR Comb Sci*. 2007;26(11-12):1211-1219. doi:10.1002/qsar.200740086
32. Agard NJ, Prescher JA, Bertozzi CR. A Strain-Promoted [3 + 2] Azide−Alkyne Cycloaddition for Covalent Modification of Biomolecules in Living Systems. *J Am Chem Soc*. 2004;126(46):15046-15047. doi:10.1021/ja044996f
33. Glassner M, Maji S, De La Rosa VR, et al. Solvent-free mechanochemical synthesis of a bicyclononyne tosylate: a fast route towards bioorthogonal clickable poly(2-oxazoline)s. *Polym Chem*. 2015;6(48):8354-8359. doi:10.1039/C5PY01280E
34. http://metabion.com. metabion. Published January 12, 2024. https://www.metabion.com/knowledge-hub/modifications/c3-azide
35. Schwetlick, Klaus. *Organikum*. 22nd ed. WILEY-VCH; 2004.
36. Hart H, Craine, Leslie E. *Organische Chemie*. Vol 3. WILEY-VCH; 2007.
37. Obushak ND, Matiichuk VS, Vasylyshin RYa, Ostapyuk YuV. Heterocyclic Syntheses on the Basis of Arylation Products of Unsaturated Compounds: X. 3-Aryl-2-chloropropanals as Reagents for the Synthesis of 2-Amino-1,3-thiazole Derivatives. *Russ J Org Chem*. 2004;40(3):383-389. doi:10.1023/B:RUJO.0000034976.75646.85
38. Hari DP, König B. The Photocatalyzed Meerwein Arylation: Classic Reaction of Aryl Diazonium Salts in a New Light. *Angew Chem Int Ed*. 2013;52(18):4734-4743. doi:10.1002/anie.201210276
39. IBM RXN for chemistry. Published September 4, 2023. https://rxn.app.accelerate.science/rxn/
40. Rossi RA, Pierini AB, Peñéñory AB. Nucleophilic Substitution Reactions by Electron Transfer. *Chem Rev*. 2003;103(1):71-168. doi:10.1021/cr960134o
41. Kazemi F, Massah AR, Javaherian M. Chemoselective and scalable preparation of alkyl tosylates under solvent-free conditions. *Tetrahedron*. 2007;63(23):5083-5087. doi:10.1016/j.tet.2007.03.083

42. Lei X, Jalla A, Abou Shama M, Stafford J, Cao B. Chromatography-Free and Eco-Friendly Synthesis of Aryl Tosylates and Mesylates. *Synthesis*. 2015;47(17):2578-2585. doi:10.1055/s-0034-1378867
43. Fazaeli R, Tangestaninejad S, Aliyan H. Solvent-free and selective tosylation of alcohols and phenols with *p* -toluenesulfonyl chloride by heteropolyacids as highly efficient catalysts. *Can J Chem*. 2006;84(5):812-818. doi:10.1139/v06-066
44. Upadhyaya DJ, Barge A, Stefania R, Cravotto G. Efficient, solventless N-Boc protection of amines carried out at room temperature using sulfamic acid as recyclable catalyst. *Tetrahedron Lett*. 2007;48(47):8318-8322. doi:10.1016/j.tetlet.2007.09.126
45. Agami C, Couty F. The reactivity of the N-Boc protecting group: an underrated feature. *Tetrahedron*. 2002;58(14):2701-2724. doi:10.1016/S0040-4020(02)00131-X
46. Sunitha S, Kanjilal S, Reddy PS, Prasad RBN. An efficient and chemoselective Brønsted acidic ionic liquid-catalyzed N-Boc protection of amines. *Tetrahedron Lett*. 2008;49(16):2527-2532. doi:10.1016/j.tetlet.2008.02.126
47. Mitchell DE, Cameron NR, Gibson MI. Rational, yet simple, design and synthesis of an antifreeze-protein inspired polymer for cellular cryopreservation. *Chem Commun*. 2015;51(65):12977-12980. doi:10.1039/C5CC04647E
48. Amine Protection and Deprotection. Master Organic Chemistry. Accessed May 1, 2024. https://www.masterorganicchemistry.com/reaction-guide/amine-protection-and-deprotection/
49. Kutonova K, Trusova M, Postnikov P, Filimonov V, Parello J. A Simple and Effective Synthesis of Aryl Azides via Arenediazonium Tosylates. *Synthesis*. 2013;45(19):2706-2710. doi:10.1055/s-0033-1339648
50. Krasavin M, Karapetian R, Konstantinov I, et al. Discovery and Potency Optimization of 2-Amino-5-arylmethyl-1,3-thiazole Derivatives as Potential Therapeutic Agents for Prostate Cancer. *Arch Pharm (Weinheim)*. 2009;342(7):420-427. doi:10.1002/ardp.200800201
51. Tabelle IR-Spektrum. sigmaaldrich. Accessed February 1, 2024. https://www.sigmaaldrich.com/AT/de/technical-documents/technical-article/analytical-chemistry/photometry-and-reflectometry/ir-spectrum-table
52. Ouchi M, Inoue Y, Liu Y, et al. Convenient and Efficient Tosylation of Oligoethylene Glycols and the Related Alcohols in Tetrahydrofuran–Water in the Presence of Sodium Hydroxide. *Bull Chem Soc Jpn*. 1990;63(4):1260-1262. doi:10.1246/bcsj.63.1260
53. Canne LE, Winston RL, Ken SBH. Synthesis of a versatile purification handle for use with Boc chemistry solid phase peptide synthesis. *Tetrahedron Lett*. 1997;38(19):3361-3364. doi:10.1016/S0040-4039(97)00651-5

8. List of Figures

9. List of Tables

10. Appendix

^{1}H-NMR compound spectra

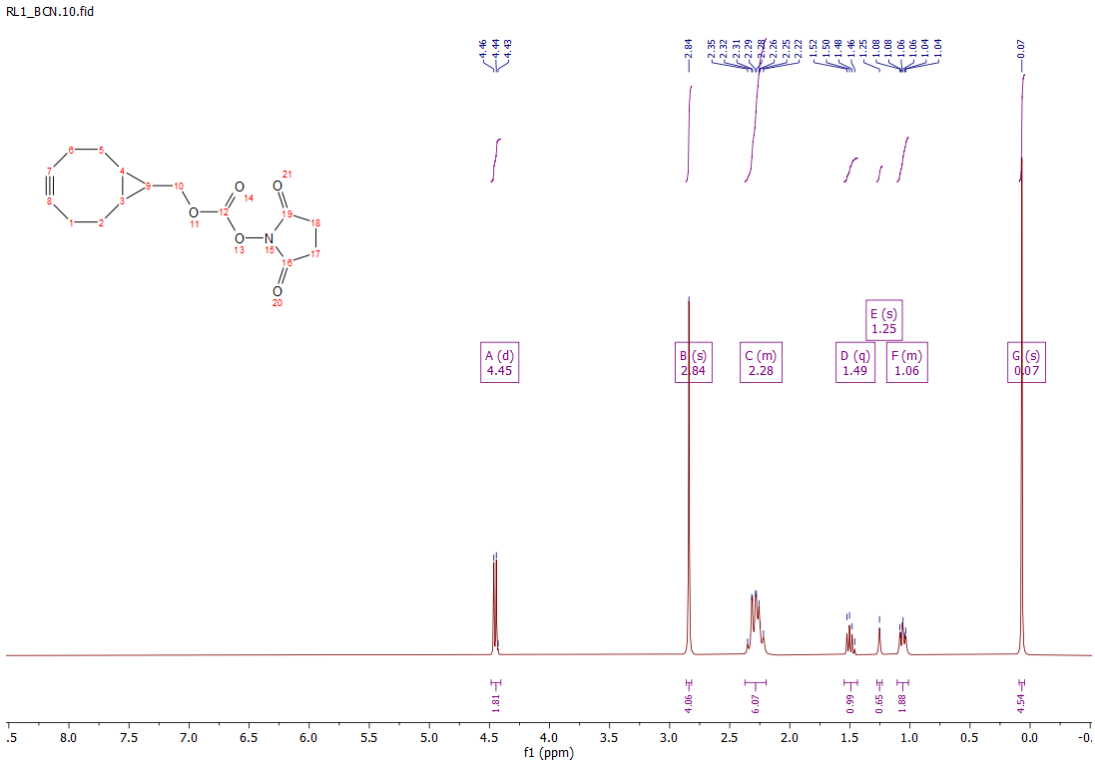

^{1}H-NMR (400 MHz, $CDCl_3$): δ (ppm) = 4.45 (d, 2H, H-10); 2.84 (s, 4H, H-17, H-18); 2.28 (m, 6H, H-1, H-2, H-5, H-6, H-7, H-8); 1.49 (q, 1H, H-9); 1.06 (m, 2H, H-3, H-4)

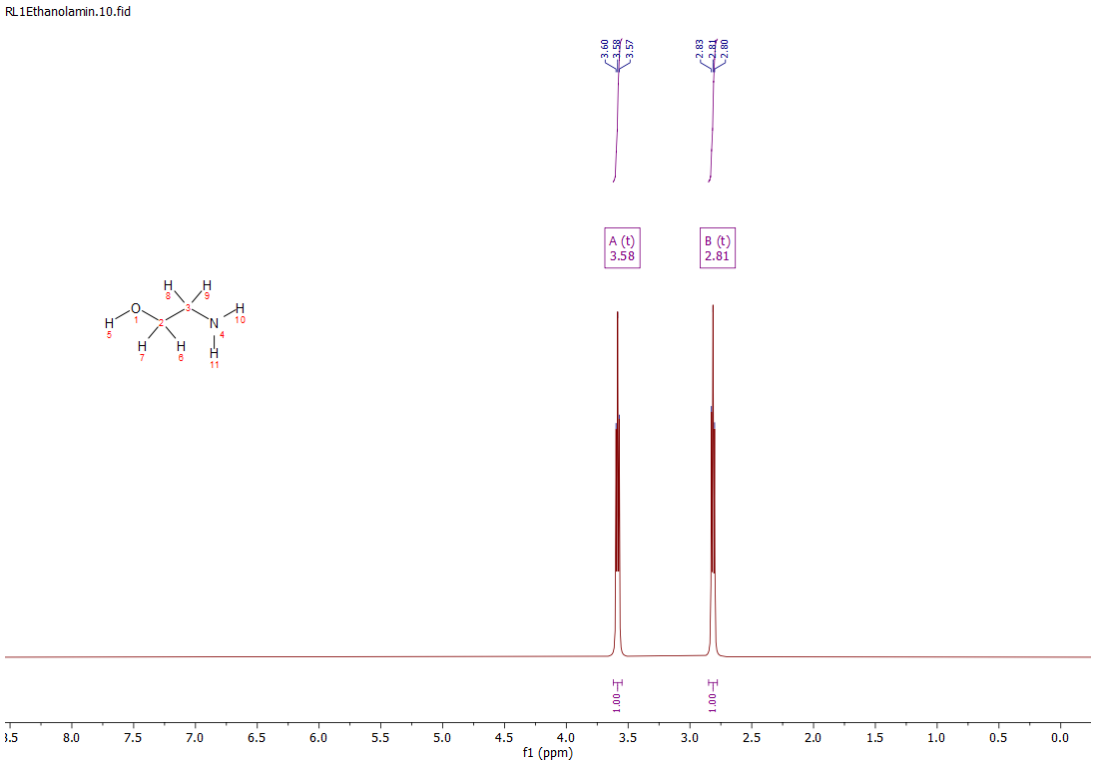

^{1}H-NMR (400 MHz, $CDCl_3$): δ (ppm) = 3.58 (t, 2H, H-6, H-7); 2.81 (t, 2H, H-8, H-9)

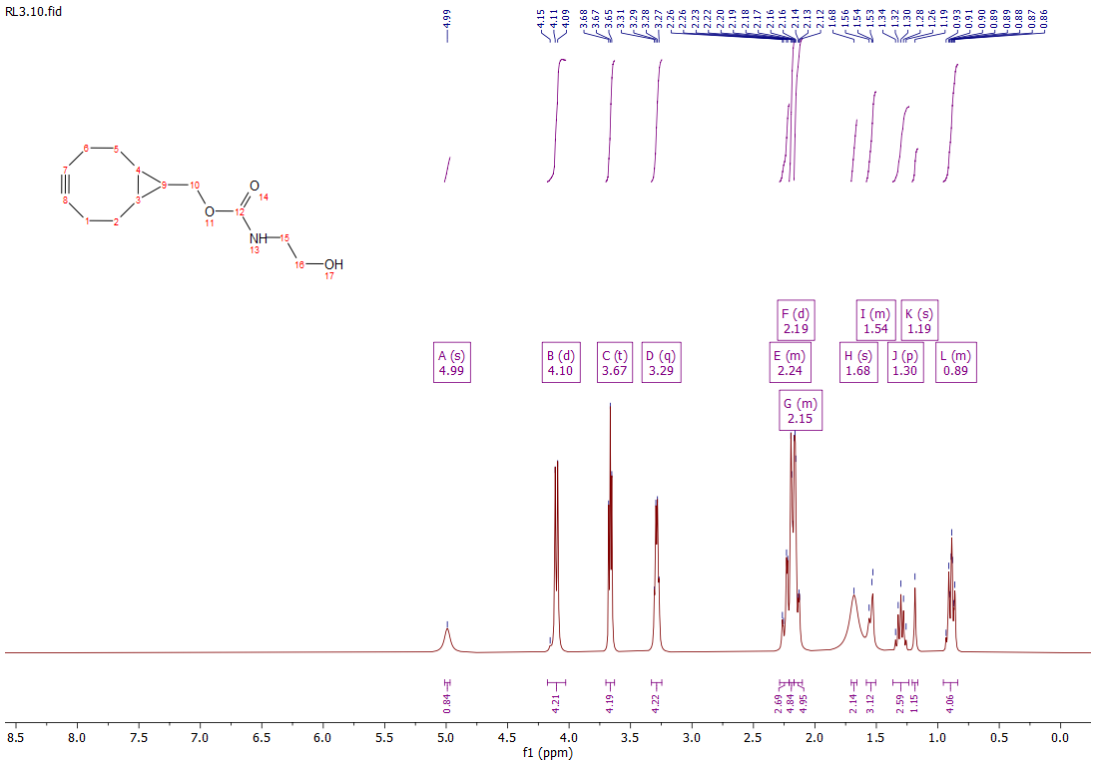

^{1}H NMR (400 MHz, $CDCl_3$): δ (ppm) = 4.99 (s, 1H, H-13); 4.10 (d, 2H, H-10); 3.67 (t, 4H, H-15, H-16); 3.29 (q, 2H, H-3, H-4); 2.24 (m, 4H, H-1, H-2, H-5, H-6); 1.54 (m, 1H, H-9)

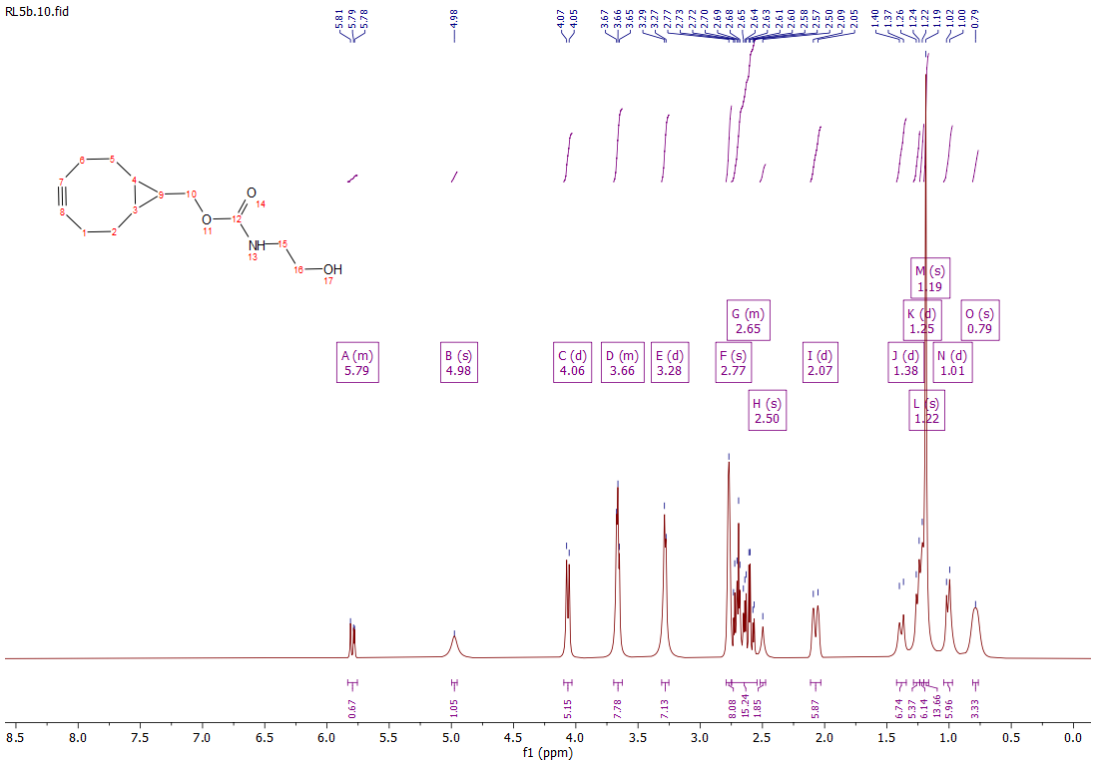

^{1}H NMR (400 MHz, $CDCl_3$): δ (ppm) = 4.98 (s, 1H, H-13); 4.06 (d, 2H, H-10); 3.66 (t, 4H, H-15, H-16); 3.28 (q, 4H, H-1, H-6); 2.65 (m, 5H, H-2, H-3, H-4, H-5, H-9)

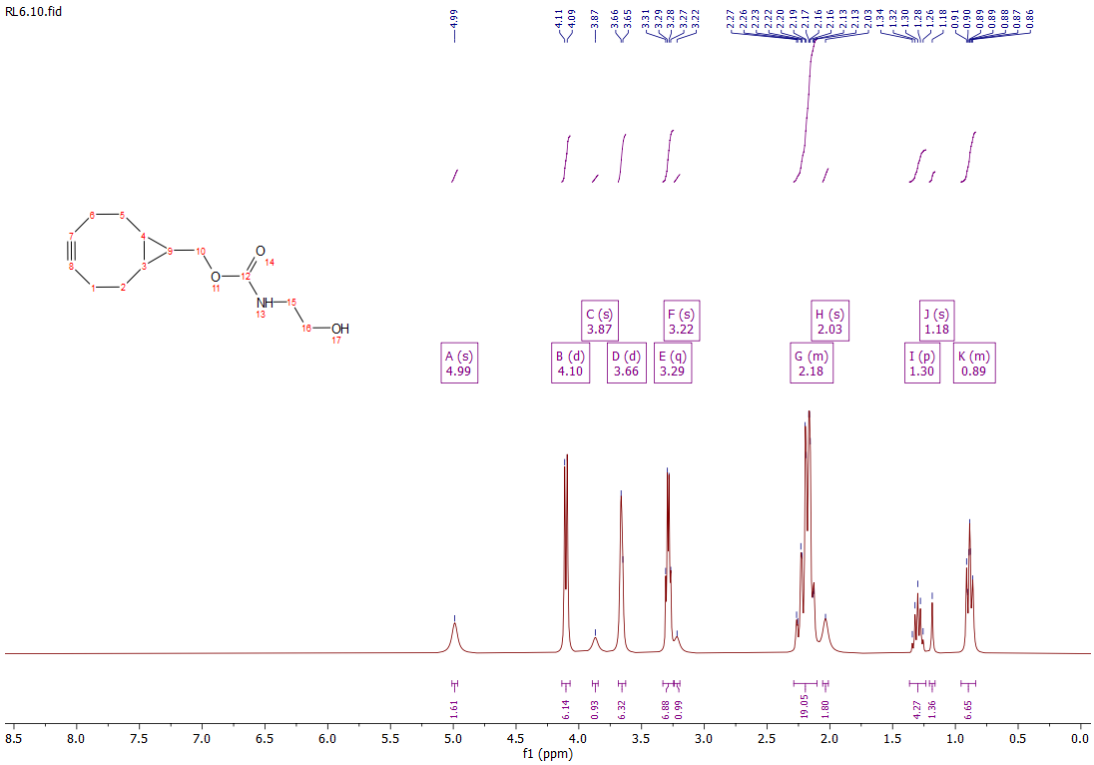

^{1}H NMR (400 MHz, $CDCl_3$): δ (ppm) = 4.99 (s, 1H, H-13); 4.10 (d, 2H, H-10); 3.26 (d, 4H, H-15, H-16); 3.29 (q, 4H, H-1, H-2, H-5, H-6); 2.18 (m, 3H, H-3, H-4, H-9)

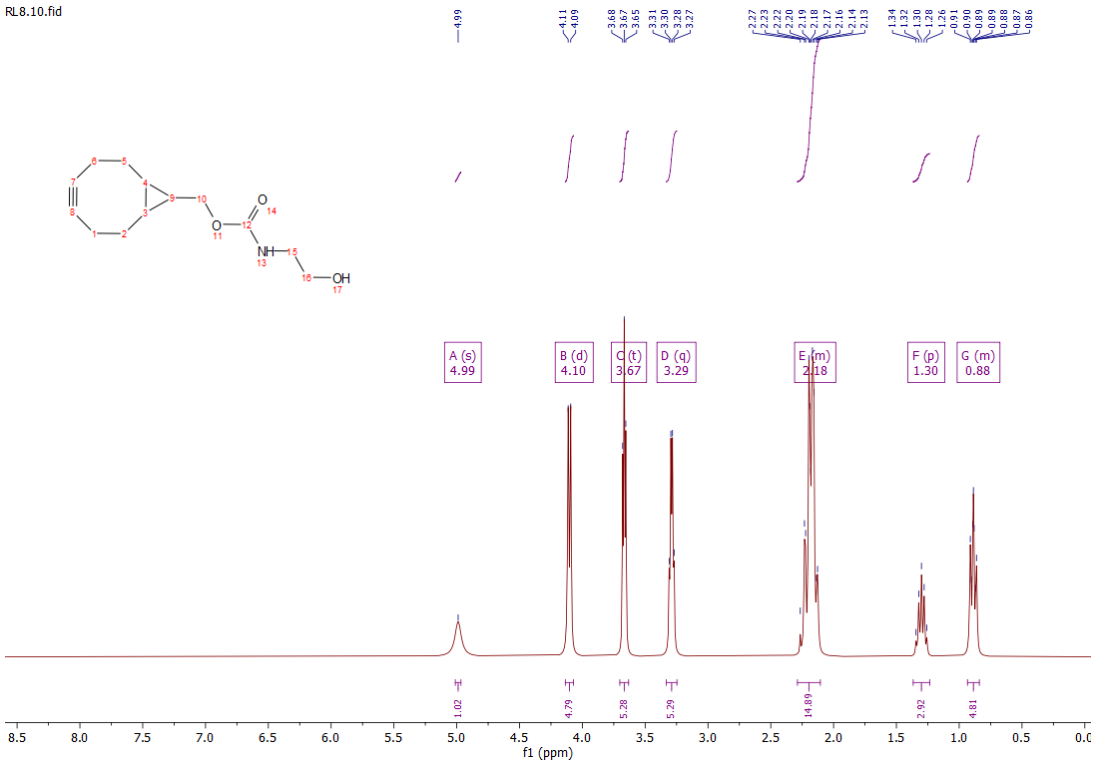

^{1}H NMR (400 MHz, $CDCl_3$): δ (ppm) = 4.99 (s, 1H, H-13); 4.10 (d, 2H, H-10); 3.67 (t, 4H, H-15, H-16); 3.29 (q, 4H, H-1, H-2, H-5, H-6); 2.18 (m, 3H, H-3, H-4, H-9)

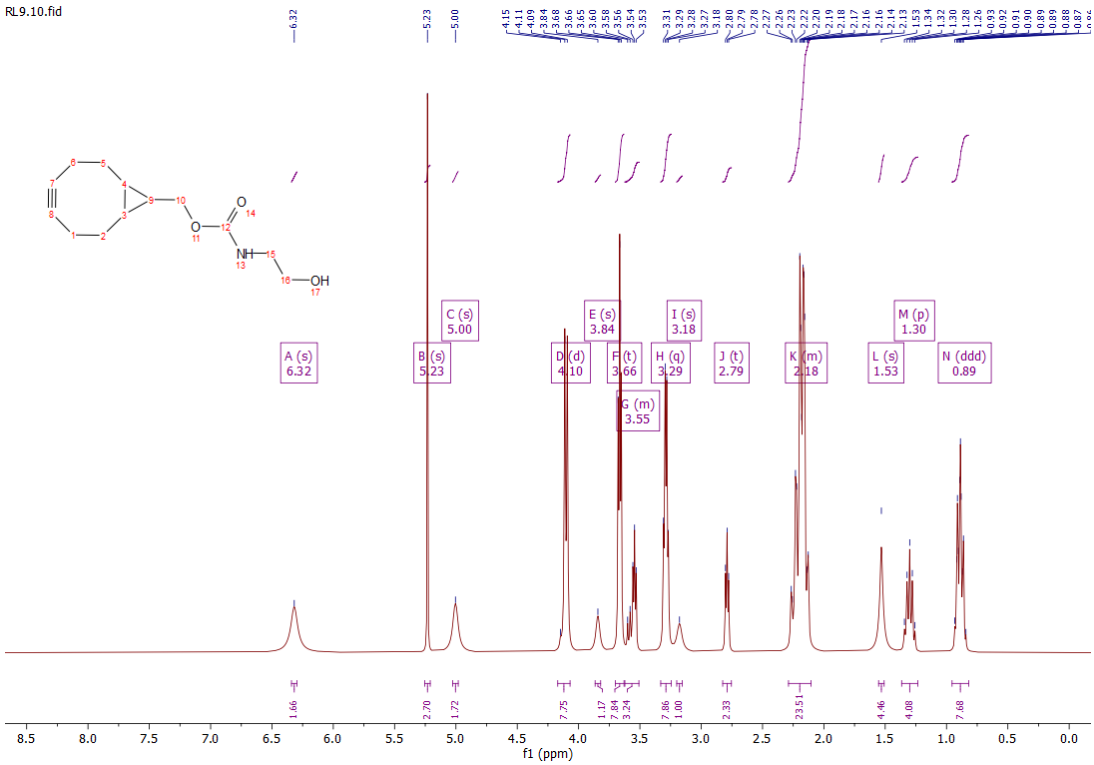

^{1}H NMR (400 MHz, $CDCl_3$): δ (ppm) = 5 (s, 1H, H-13); 4.10 (d, 2H, H-10); 3.66 (t, 4H, H-15, H-16); 3.29 (q, 4H, H-1, H-2, H-5, H-6); 2.18 (m, 3H, H-3, H-4, H-9)

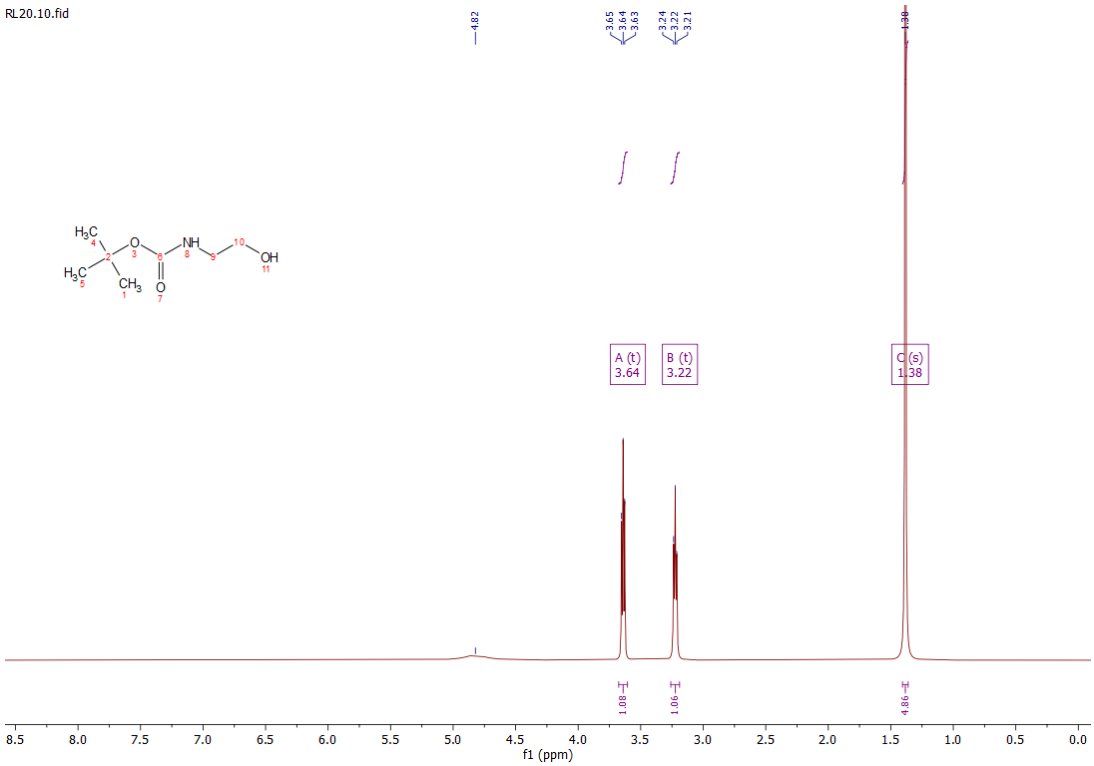

^{1}H-NMR (400 MHz, $CDCl_3$): δ (ppm) = 3.64 (t, 2H, H-10); 3.22 (t, 2H, H-9); 1.38 (s, 9H, Boc-CH_3)

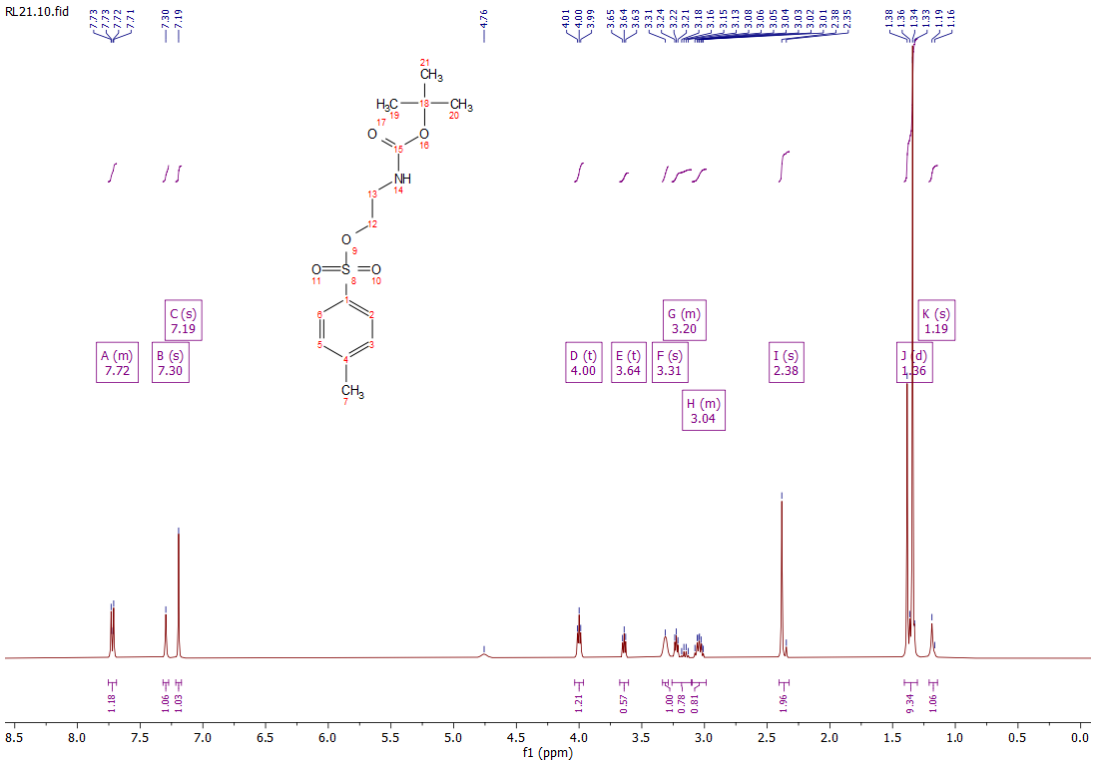

^{1}H NMR (400 MHz, $CDCl_3$): δ (ppm) = 7.72 (m, 4H, H-2, H-3, H-5, H-6); 4.75 (H-14, N-H); 4.00 (t, 2H, H-12); 3.64 (t, 2H, H-13); 2.38 (s, 3H, H-7); 1.36 (d, 9H, Boc-CH_3)

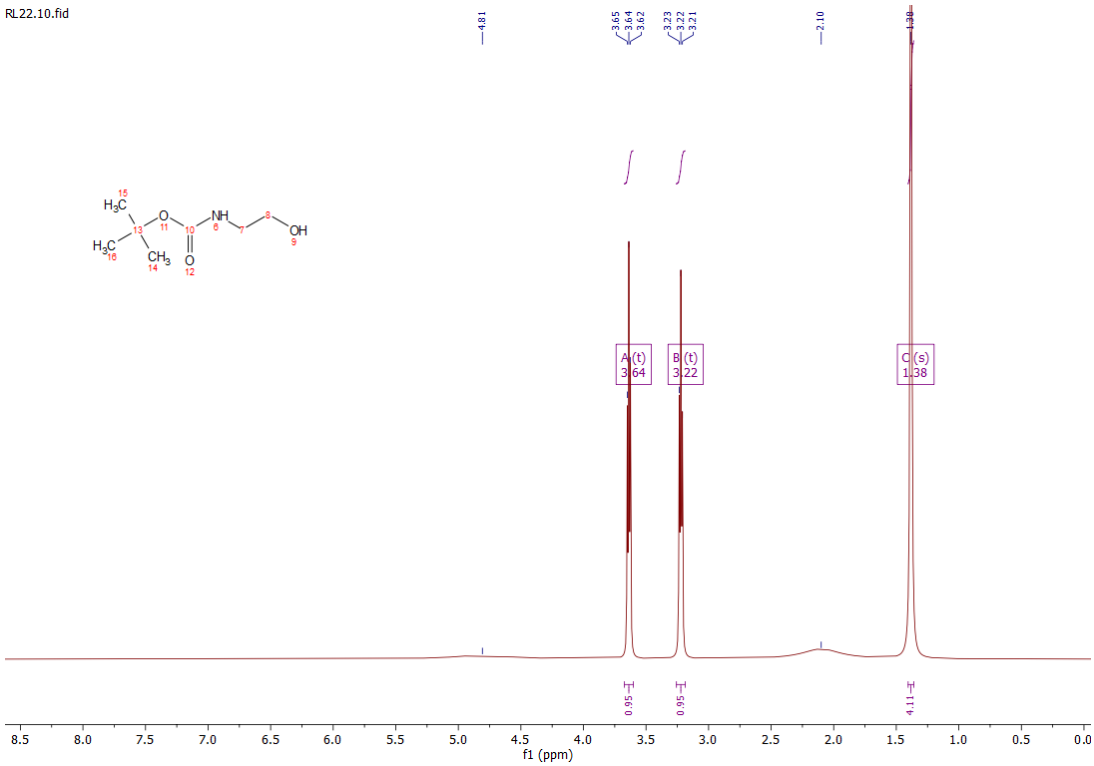

^{1}H-NMR (400 MHz, $CDCl_3$): δ (ppm) = 4.81 (N-H); 3.64 (t, 2H, H-10); 3.22 (t, 2H, H-9); 1.38 (s, Boc-CH_3)

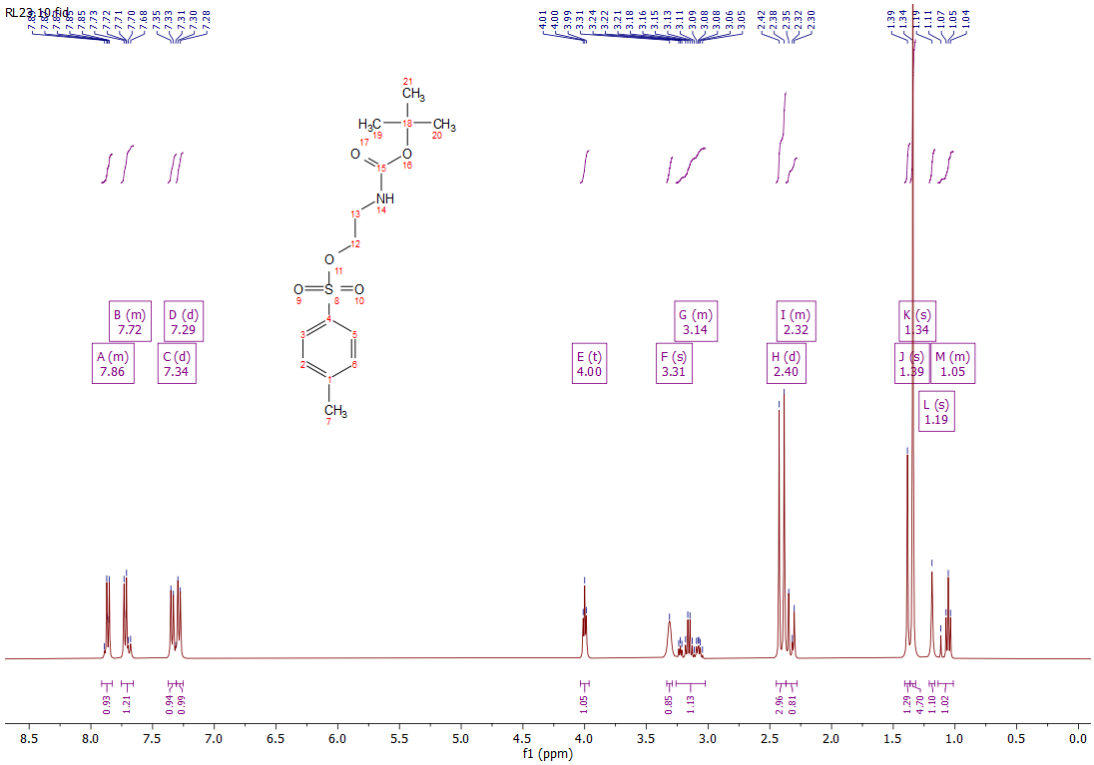

^{1}H NMR (400 MHz, $CDCl_3$): δ (ppm) = 7.86 (m, 2H, H-3, H-5) 7.72 (m, 2H, H-2, H-6); 4.00 (t, 2H, H-12); 3.14 (m, 2H, H-13); 1.39 (s, 3H, H-7); 1.34 (s, 9H, Boc-CH_3)

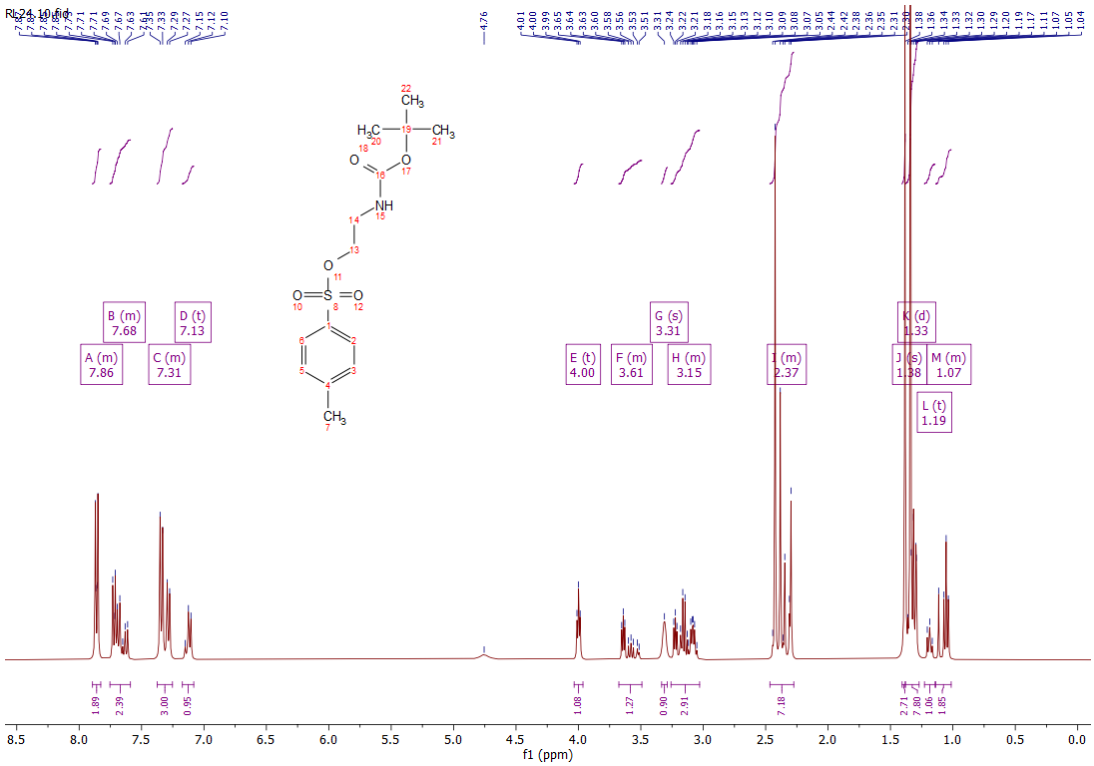

^{1}H NMR (400 MHz, $CDCl_3$): δ (ppm) = 7.86 (m, 2H, H-2, H-6) 7.68 (m, 2H, H-3, H-5); 4.76 (H-15, N-H); 4.00 (t, 2H, H-13); 3.15 (m, 2H, H-14); 1.38 (s, 3H, H-7); 1.33 (d, 9H, Boc-CH_3)

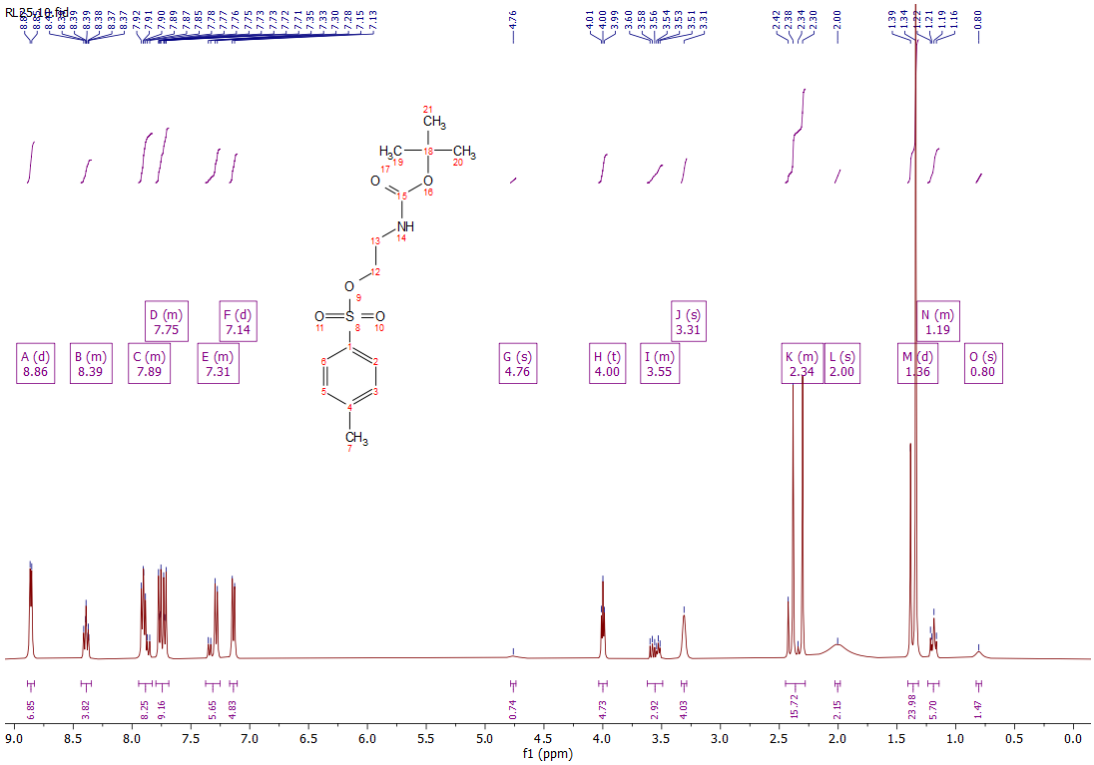

^{1}H NMR (400 MHz, $CDCl_3$): δ (ppm) = 7.89 (m, 2H, H-2, H-6) 7.75 (m, 2H, H-3, H-5); 4.76 (H-14, N-H); 4.00 (t, 2H, H-12); 3.55 (m, 2H, H-13); 2.00 (s, 3H, H-7); 1.36 (d, 9H, Boc-CH_3)

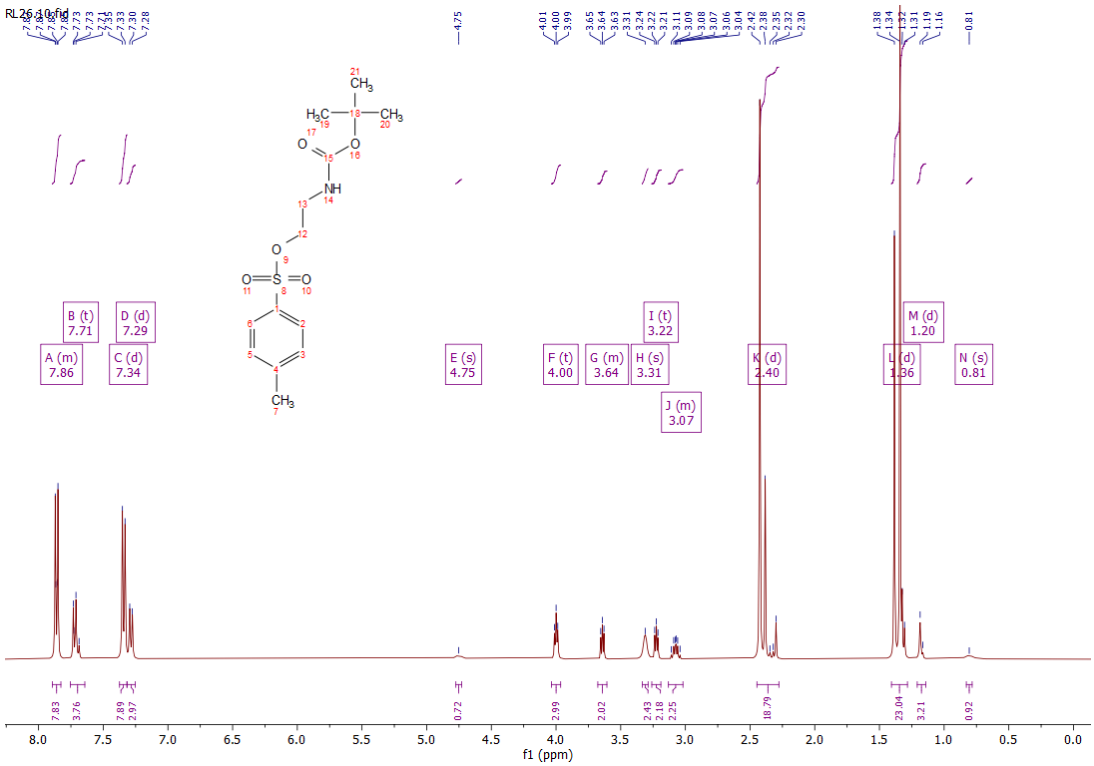

^{1}H NMR (400 MHz, $CDCl_3$): δ (ppm) = 7.86 (m, 2H, H-2, H-6) 7.71 (t, 2H, H-3, H-5); 4.75 (H-14, N-H); 4.00 (t, 2H, H-12); 3.46 (m, 2H, H-13); 3.31 (s, 3H, H-7); 1.36 (d, 9H, Boc-CH_3)

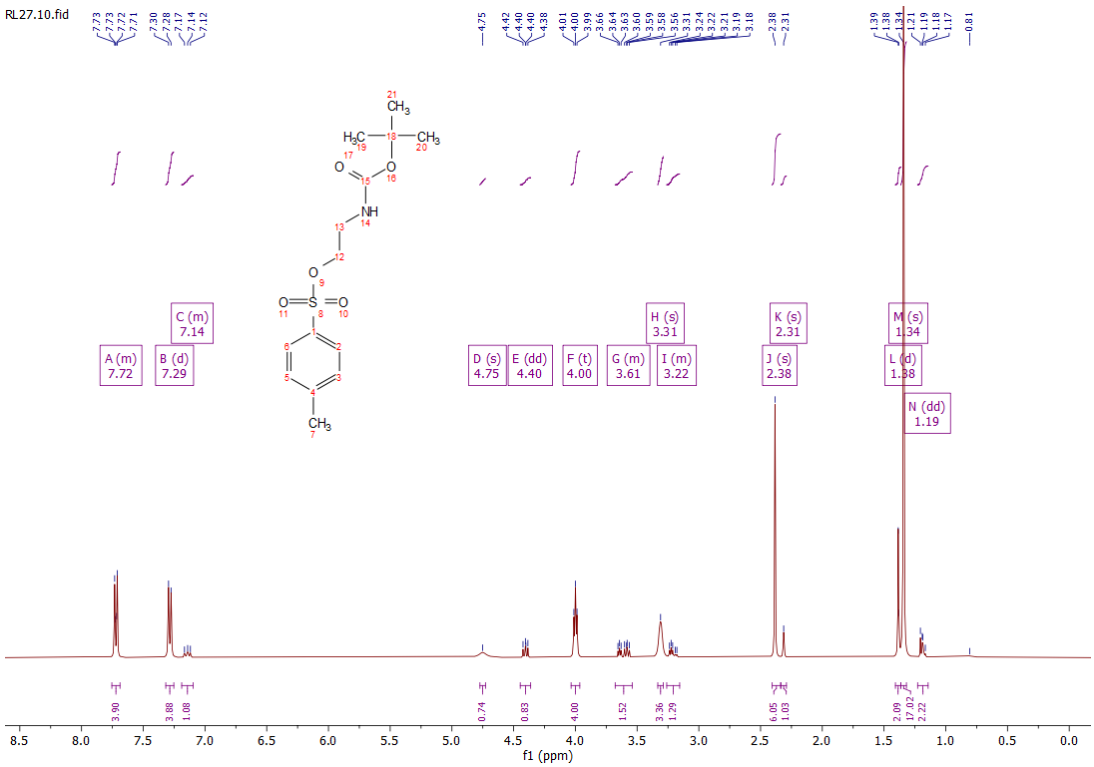

^{1}H NMR (400 MHz, $CDCl_3$): δ (ppm) = 7.72 (m, 4H, H-2, H-3, H-5, H-6); 4.75 (H-14, N-H); 4.00 (t, 2H, H-12); 3.61 (m, 2H, H-13); 2.38 (s, 3H, H-7); 1.33 (s, 9H, Boc-CH_3)

Mass spectra

RL21

2-tert-butoxycarbonylamino)ethyl-4-methylbenzenesulfonate

HRMS (ESI): (m/z) = $[M + Na]^+$ calculated for $C_{14}H_{21}NNaO_5S$: 338.1033, found: 338.1046

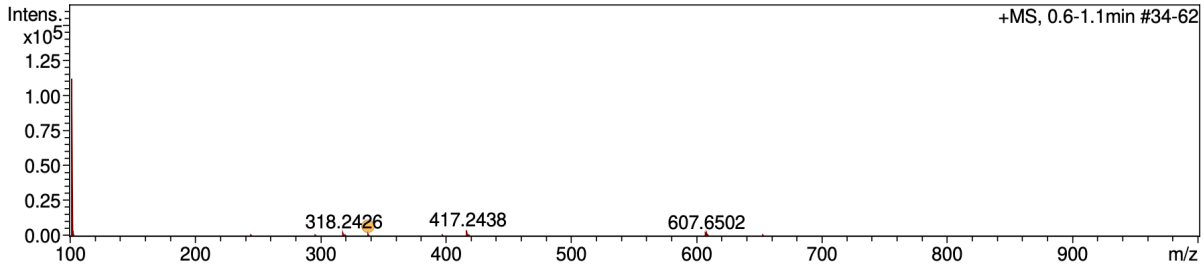

RL22

2-(N-tert-butoxycarbonylamino)ethanol

HRMS (ESI): (m/z) = $[M + Na]^+$ calculated for $C_7H_{15}NNaO_3$: 184.099, found: 184.0956

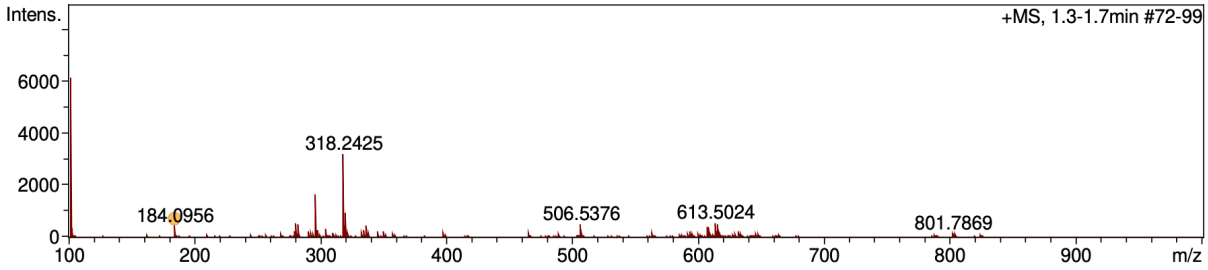

RL23

2-tert-butoxycarbonylamino)ethyl-4-methylbenzenesulfonate

HRMS (ESI): (m/z) = $[M + Na]^+$ calculated for $C_{14}H_{21}NNaO_5S$: 338.1033, found: 338.1044

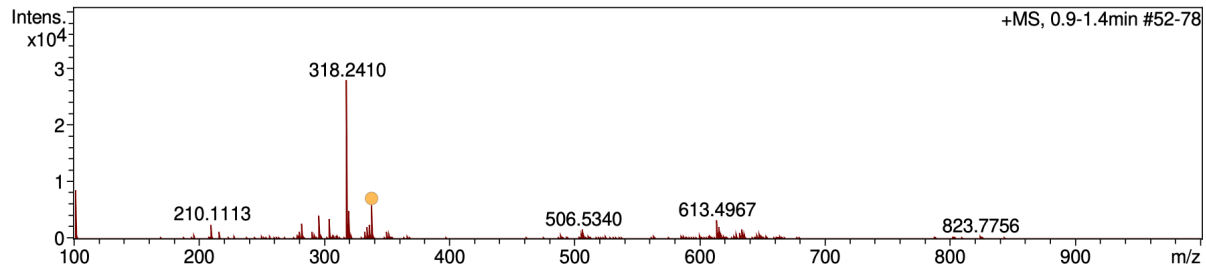

RL24

2-tert-butoxycarbonylamino)ethyl-4-methylbenzenesulfonate

HRMS (ESI): (m/z) = $[M + Na]^+$ calculated for $C_{14}H_{21}NNaO_5S$: 338.1033, found: 338.108

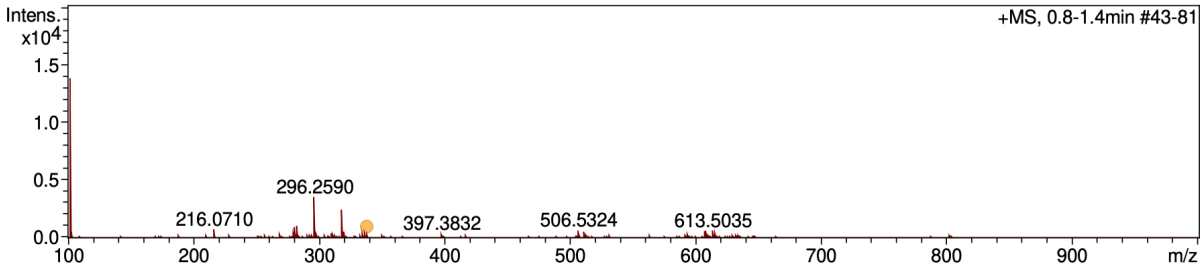

RL25

2-tert-butoxycarbonylamino)ethyl-4-methylbenzenesulfonate

HRMS (ESI): (m/z) = $[M + Na]^+$ calculated for $C_{14}H_{21}NNaO_5S$: 338.1033, found: 338.1092

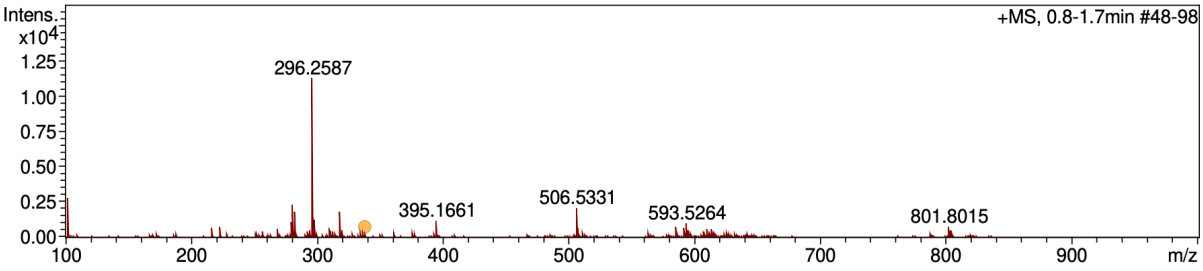

RL26

2-tert-butoxycarbonylamino)ethyl-4-methylbenzenesulfonate

HRMS (ESI): (m/z) = $[M + Na]^+$ calculated for $C_{14}H_{21}NNaO_5S$: 338.1033, found: 338.1091

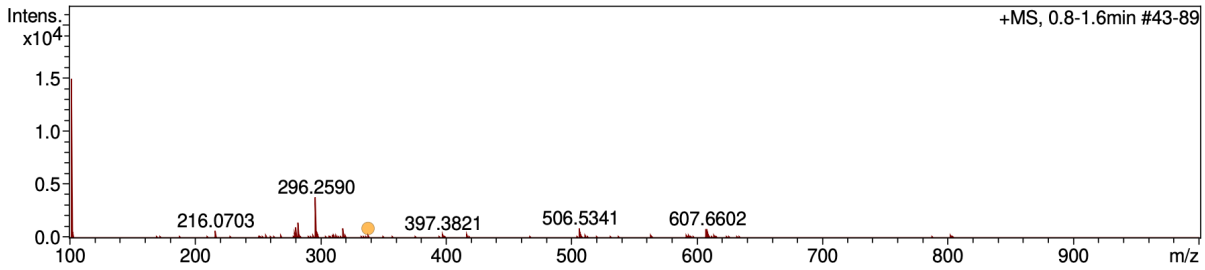

RL 27

2-tert-butoxycarbonylamino)ethyl-4-methylbenzenesulfonate

HRMS (ESI): (m/z) = $[M + Na]^+$ calculated for $C_{14}H_{21}NNaO_5S$: 338.1033, found: 338.104

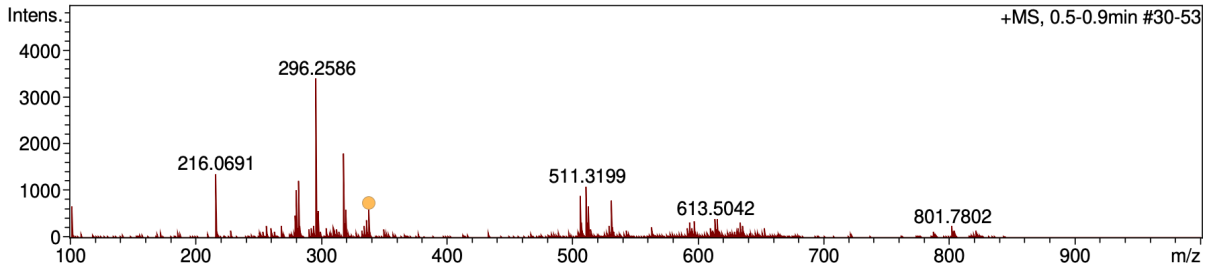

IR spectra

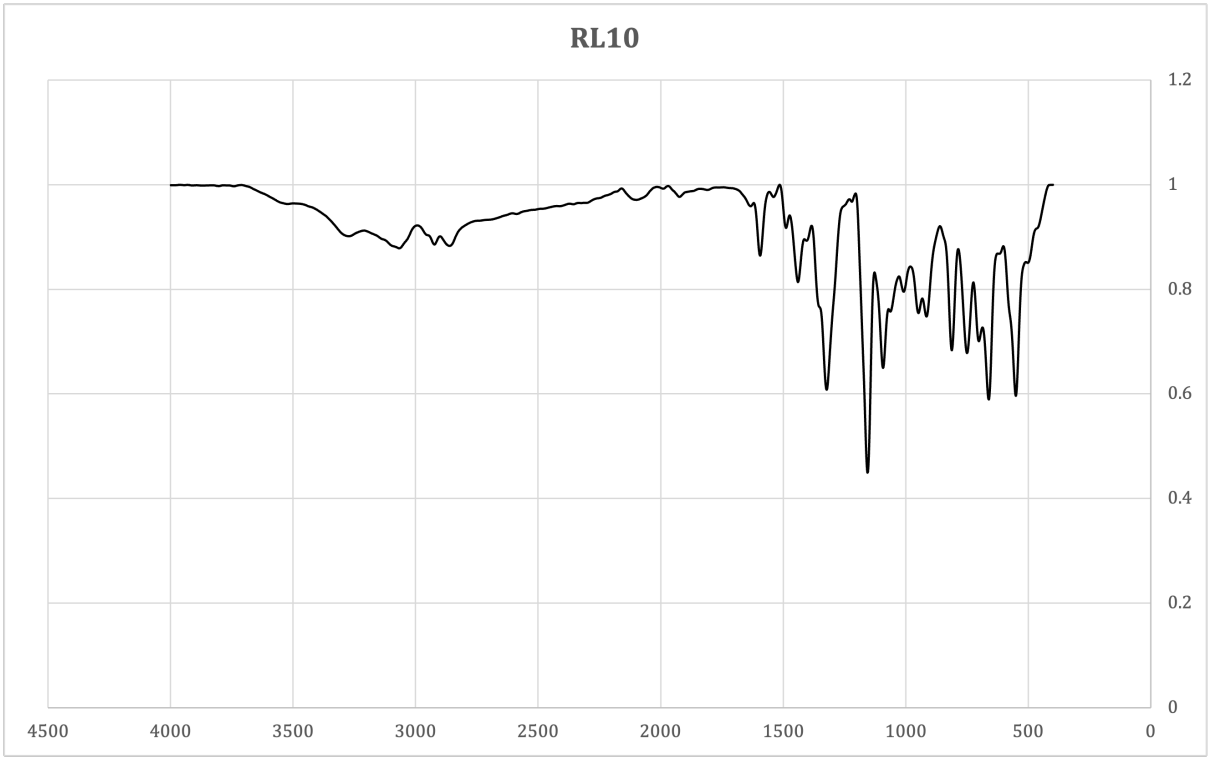

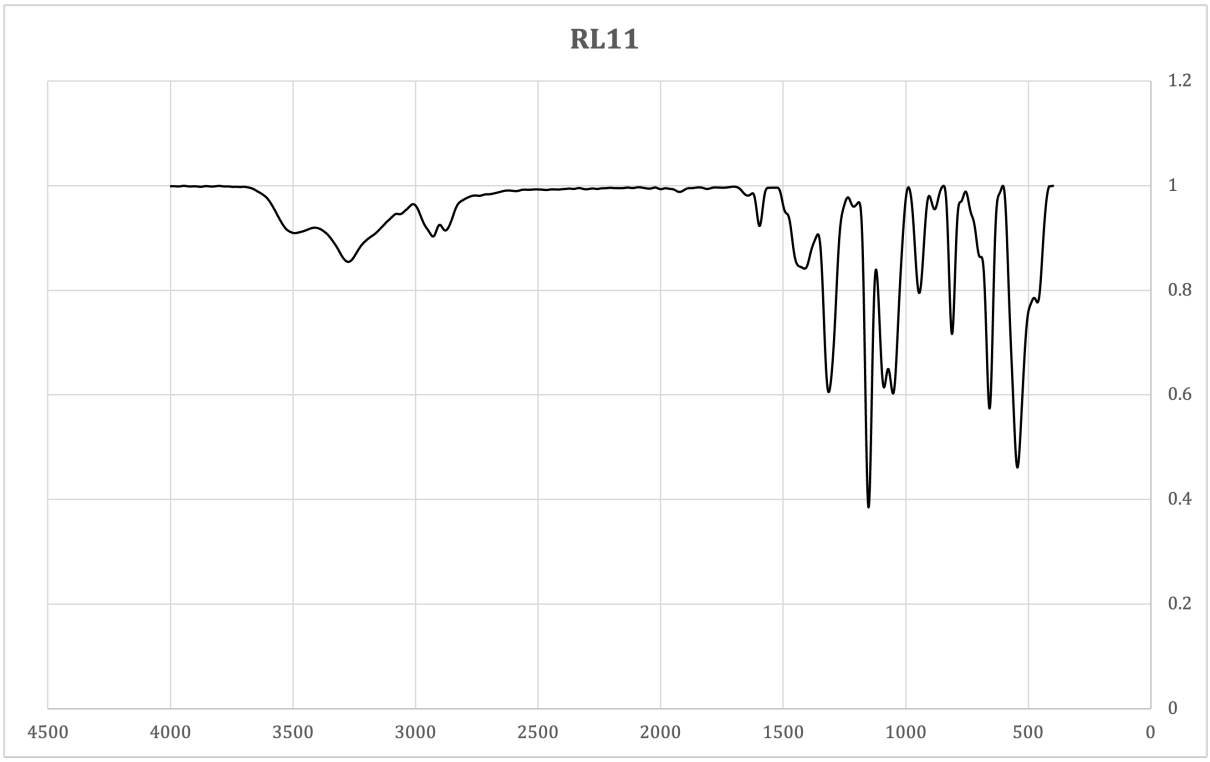
RL11
1.2
1
0.8
0.6
0.4
0.2
0
4500
4000
3500
3000
2500
2000
1500
1000
500
0

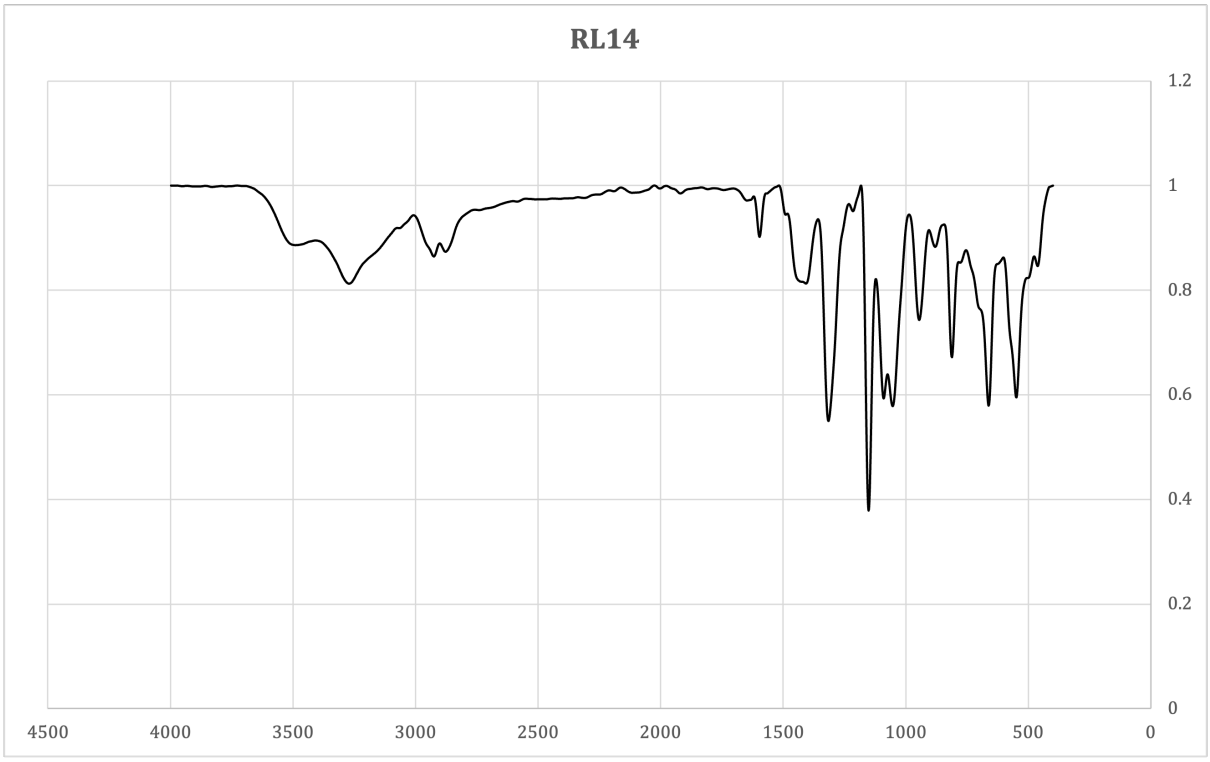
RL14
1.2
1
0.8
0.6
0.4
0.2
0
4500
4000
3500
3000
2500
2000
1500
1000
500
0

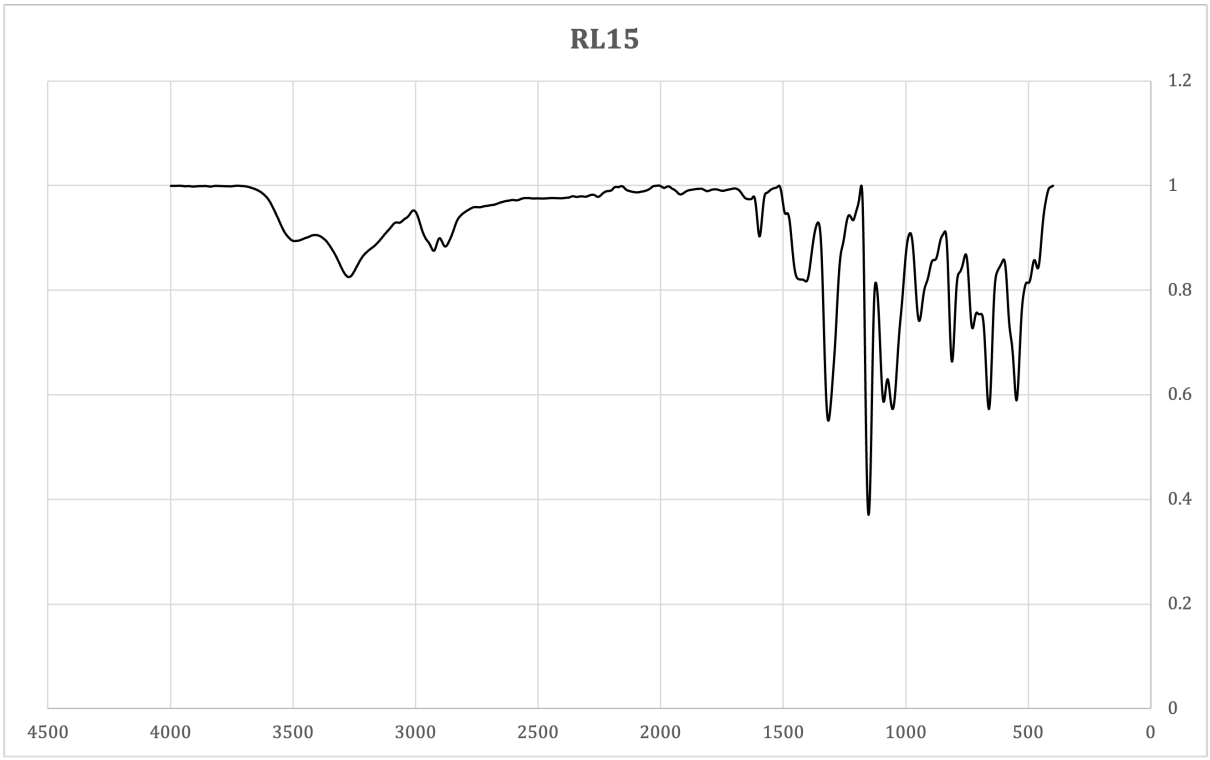
RL15
1.2
1
0.8
0.6
0.4
0.2
0
4500
4000
3500
3000
2500
2000
1500
1000
500
0

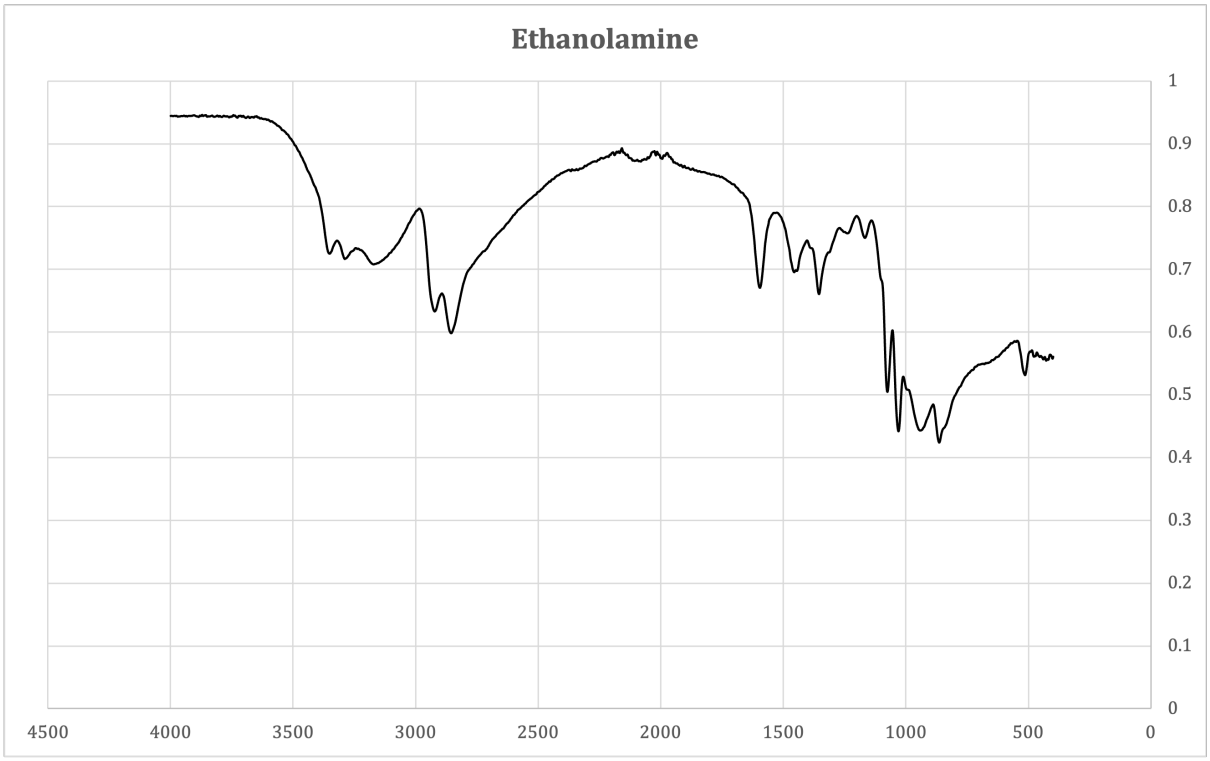
Ethanolamine
1
0.9
0.8
0.7
0.6
0.5
0.4
0.3
0.2
0.1
0
4500
4000
3500
3000
2500
2000
1500
1000
500
0

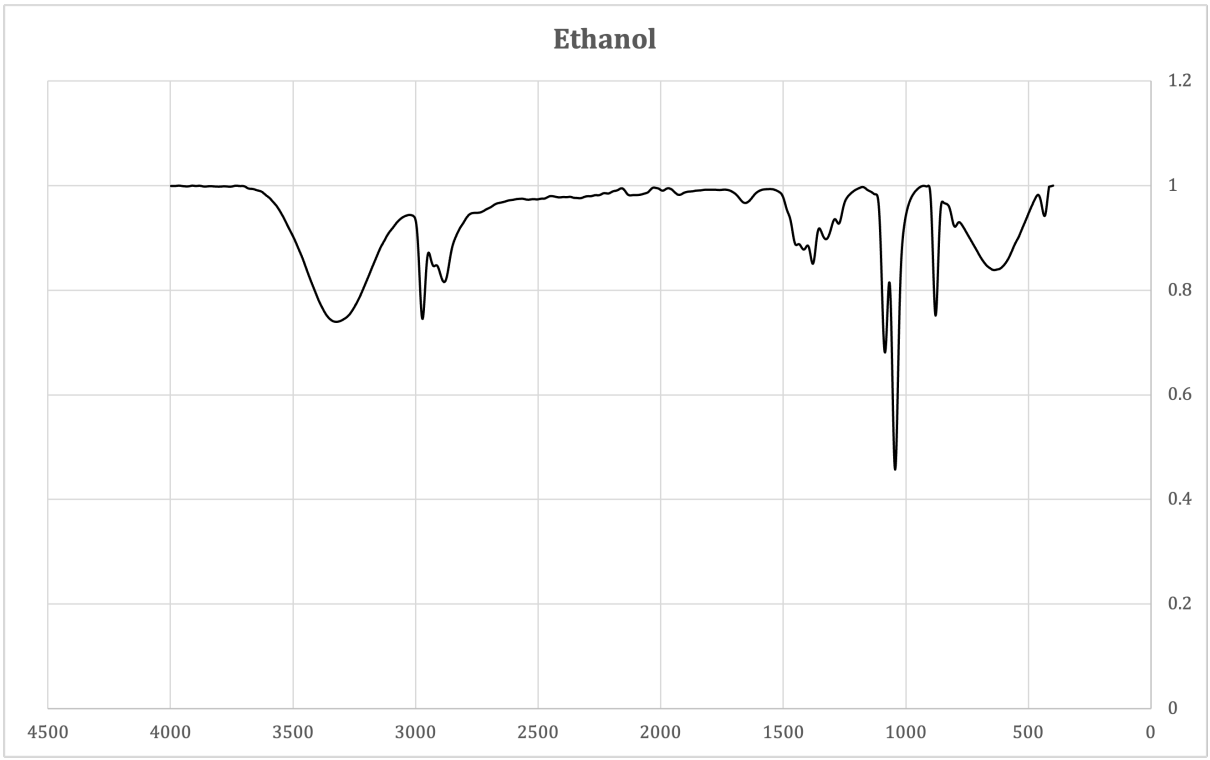
Ethanol
1.2
1
0.8
0.6
0.4
0.2
0
4500
4000
3500
3000
2500
2000
1500
1000
500
0

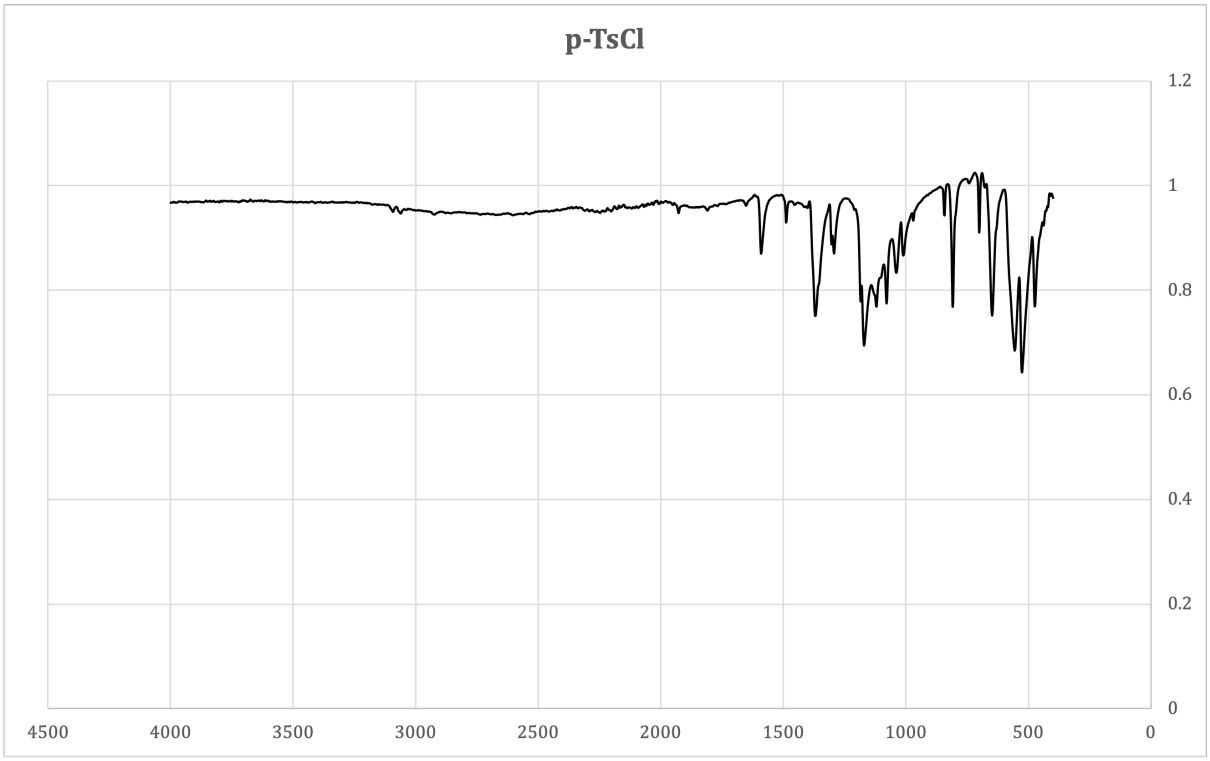
p-TsCl
1.2
1
0.8
0.6
0.4
0.2
0
4500
4000
3500
3000
2500
2000
1500
1000
500
0